Biomimetic Vascular Networks for Self-Healing Concrete

by
Charles Kimber (EM)

Fourth-year undergraduate project
in Group D, 2013/2014

I hereby declare that, except where specifically indicated, the work submitted herein is my own original work.

Signed: ______________ Date: 28/05/2014

Biomimetic Vascular Networks for Self-Healing Concrete

by Charles Kimber (EM)
Group D 2013/2014

Technical Abstract

Concrete is one of mankind's most widely used materials by weight, coming second only to water. 8 cubic kilometres of it are produced globally each year; enough to fill the Panama Canal almost twice over. Portland cement, one of the primary constituents of concrete, is also environmentally "dirty", contributing 7% to global carbon emissions. Clearly, any scalable process which significantly improves the cost or sustainability of concrete could have a large effect globally.

The material properties of concrete mean that it is strong in compression and very weak in tension. Weight-efficient concrete structural elements are therefore designed with their tensile side reinforced, usually by steel. Cracking still occurs on the tensile side, but the width is controlled by compatibility constraints imposed by the reinforcement.

Cracking becomes a problem if the cracks are allowed to grow, exposing the reinforcement to atmospheric conditions. If water is allowed to pervade the cracks it can cause corrosion of the steel, compromising the overall integrity of the structure. For this reason, concrete requires regular maintenance and repair; an expensive operation contributing 45% of UK construction costs.

Self-healing concrete is explored here as a solution to the problem of cracking in concrete, particularly bioinspired designs that mimic vascular healing in natural materials. The concept involves delivering a healing agent through a material's internal structure and transporting it to the point of damage, in order to seal the crack against ingress of aggressive substances and recover the material's strength and stiffness.

A comprehensive literature review is presented, evaluating the state-of-the-art in the field of self-healing concrete, with a particular focus on tubular encapsulation of healing agent. It was found that interconnected vascular healing methods developed for self-healing polymers and composites have not yet been widely explored in cementitious materials, despite some success with simpler systems employing discrete tubes to deliver healing agent to the damage site. Desired attributes of self-healing materials were identified and used as a framework for analysing success of designs.

A 3D printer was used to construct networks of the structural polymer Polylactic Acid (PLA). Tests on printed tubes revealed that their material properties are highly dependent on their orientation during the printing process. Connections between printed layers are weak in tension and fracture in a brittle manner, while parts can carry tension parallel to these planes well. Tubes were therefore printed vertically, with their fracture plane perpendicular to the axis

of the tube.

Tests on tubes in isolation revealed that the Young's modulus of PLA tubes extruded in layers by a 3D printer increases by between 50 and 300%. It was noted that inaccuracies in the tubes' second moment of area may have contributed to the wide spread of results, but also that the stiffness was qualitatively increased, and strain-to-failure reduced, by printing tubes in this manner when compared to the isotropic material properties of PLA.

3D printed tubes and networks were cast in small reinforced prismatic mortar beams, protruding from each end so that fluid was free to flow through the assembly. When tested in three-point bending, these tubes and networks were found to reliably fracture in the same location as the surrounding mortar and release fluid into the crack, proving the concept of vascular healing in concrete using 3D printed components.

When various healing agents were pumped through the tubes, migration was observed at the crack face in the majority of cases, and it was possible to fill the cracks. However, strength and stiffness recovery was generally poor for these specimens. It is thought that the reason for this is the large observed crack width at first leakage, causing poor adhesion between crack faces and pointing to tensile failure of the reinforcement.

Finally, an interconnected network design was printed and cast in the same reinforced mortar specimens. The networks were filled with two cyanoacrylate-based adhesives with different viscosities (3 cPs and 100 cPs). Strength recovery of up to 52% in the high viscosity samples, and 60% in the low viscosity samples, was observed after 24 hours healing, rising to 72% and 65% respectively in tests conducted after 48 hours. The stiffness recovery was 69 - 77% in high viscosity samples and 74 - 100% in low viscosity samples, a significant improvement on controls and the tests performed on unconnected tubes.

The reason for this improvement is thought to be the reduced crack width required to force fluid leakage from cracks in the vascular networks. Because of the small length scales within the network, viscous forces on the fluid are significant, and scale with the length of the channel traversed. The interconnected network design contained tubular loops. When one of these loops is broken, the effective channel length is reduced and consequently so are resistive forces on the fluid. The networks also cracked sooner after the concrete than the individual tubes did, because their greater width resulted in an increased second moment of area and therefore bending stiffness.

Cyanoacrylate is not an ideal healing agent as it solidifies when air reaches the cracked network, meaning that only one healing cycle is possible in this experimental configuration. Considering the complexity of the set-up, this limits the concept's utility outside of the lab. However, vascular networks have shown promise in self-healing for cementitious materials. Strength and stiffness recovery compared to controls were demonstrated and reliable leakage at small crack widths was achieved. Further work should focus on finding a repeatable mechanism for healing as well as improving strength and stiffness recovery to above 100%.

Contents

1 Introduction

1.1 Motivation

The built environment is dominated by concrete. Civil engineering's roads, infrastructure, tallest buildings and longest bridges are all made possible by this strong, cheap, adaptable granular composite. It is the world's most widely used man-made material, with over a cubic metre per person produced annually [1].

However, cementitious materials (of which concretes are a subset) are weaker in tension than compression by orders of magnitude. For this reason, the tensile sides of concrete beams are reinforced with steel bars, which carry the additional tensile loads where the concrete cannot.

Microcracks are an unavoidable feature of untreated concrete, arising from shrinkage, loading, expansion and creep [2]. These cracks do not pose a problem if they are carefully managed, but tend to expand and propagate over the life of the structure, accelerating with time. Combined with the inherent porosity of concrete, these growing microcracks can form a network, allowing ingress of aggressive substances, particularly water, which contribute to further erosion [3]. Moreover, if the crack network is allowed to reach the reinforcement, ingress of water will corrode the steel, and the subsequent reduction in tensile strength could lead to catastrophic failure of the structure.

1.1.1 Concrete Maintenance Economics

This microcracking property of concrete means that it regularly requires repair and maintenance. Around 45% of the activity of the UK construction industry is involved in maintenance, repair, upgrading and monitoring of existing structures [4]. It has long been known that paying for higher initial quality work can result in lower lifetime cost of a structure after repair and maintenance work has been taken account of. Ideal self-healing materials take this idea one step further: if it were possible to create a structure which reliably reverses any damage it undergoes, the lifetime cost could *exactly equal* the total cost of construction (see figure 1).

This simplified model does not take the effects of interest and inflation into account, but does illustrate that increased up-front cost for a self-healing structure could be a viable financial decision for owners of long-life structures. Furthermore, if the repair is initiated automatically and repeatedly as a result of some damage signal (figure 1(c)), the safety margin on the required strength will remain larger than it would if repairs are delayed until the structure is close to failure (figure 1(a)). This reduces the probability of failure in extreme load cases, which may occur if a structure is already damaged.

1.1.2 Carbon Emissions

Portland cement (PC) is the overwhelmingly dominant binder used in concrete. Over 2 gigatons of it is produced each year, contributing around 7% to global direct carbon emissions

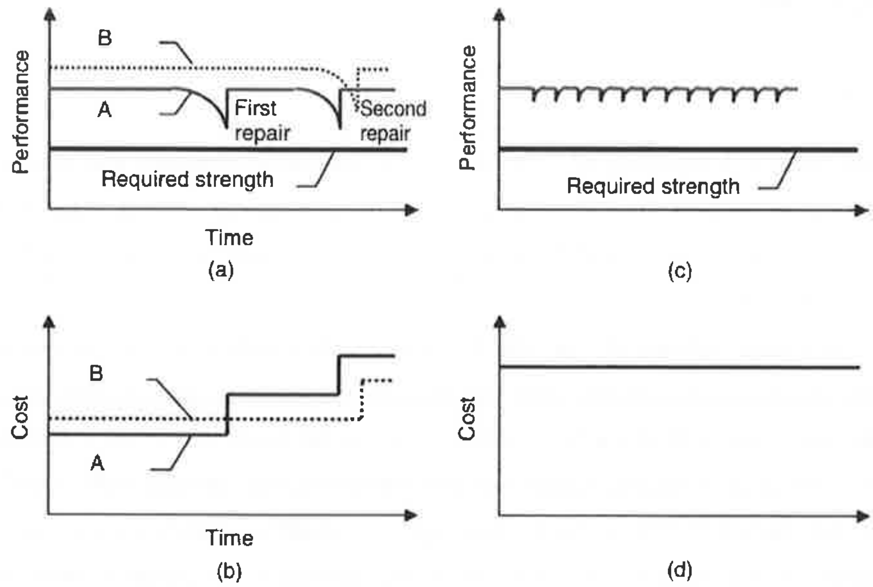

Figure 1: *Economics of self-healing structures. (a) & (b): Higher initial up-front costs can result in lower total costs for long-life structures. A higher quality structure (dashed line B) will require fewer repairs than a lower quality structure (solid line A), whose total cost may over take that of a higher quality structure in the long term. (c) & (d): An ideal self-healing structure does not need to be repaired, so the total cost is equal to initial cost. In the long term, this will always be economically advantageous. (from [5]).*

through the calcination and kiln heating processes. Moreover, the emissions associated with steel reinforcement production substantially increase the carbon footprint of complex concrete structures [5]. Additionally, rapid expansion of developing economies (particularly China and India) means that demand for concrete in construction is expected to double by 2050 [6].

Clearly, self-healing concrete is not going to solve the problem of this increased demand for new buildings. However, with similar reasoning to that applied earlier to economic costs, by reducing the cement usage in repair and maintenance, the lifetime carbon footprint of concrete structures could be reduced by automated repair systems. If so many new structures are to be built, it would be environmentally advantageous to build them in a sustainable, forward-thinking manner.

1.2 Aims and Objectives

This project aimed to explore the feasibility of using vascular networks (embedded hollow arrays which transport a healing agent to the region of damage) for self-healing in concrete. The key objectives were therefore to:

- conduct a thorough literature review of self-healing materials, with a particular focus on self-healing concrete, vascular networks, and the combination of the two;

- assess the specific properties of concrete which affect the design of vascular networks for self-healing in such a complex material;
- develop a means of constructing vascular networks that enable self-healing in concrete;
- investigate the flow of healing agent through the networks;
- develop a means of casting concrete around the vascular networks, keeping them in place and ensuring blockages do not occur;
- investigate the self-healing performance of the vascular specimens.

1.3 Report Outline

This report is divided into 5 sections. Section 1 introduces the project, discussing its motivation and providing some background on self-healing concrete. Section 2 is a literature review of vascular networks for self-healing and self-healing in concrete, in which key terms are defined and areas requiring further research are highlighted. Section 3 gives a detailed exploration of each experimental set-up: the materials and methods used and highlighting what the tests were attempting to achieve and quantify. Section 4 presents the results and discusses what they show, and section 5 draws conclusions from the observations and suggests a direction for future research in the area. Finally, the References are listed and supplementary material is presented in the Appendix.

2 Literature Review

This section summarises the relevant developments in self-healing materials over the last few decades. Initial progress was made in self-healing materials for civil engineering throughout the 1990s. However, more work was undertaken in self-healing polymers for electronics and composite panels for aerospace in the early 21st Century, possibly as a result of reduced constraints on funding for research with military applications. Self-healing construction materials have returned to the fore recently with heightened political and public interest in sustainability in the built environment.

Some key terminology has been defined following the first international conference on self-healing materials in 2007 [7]. This is presented first, followed by an overview and discussion of developments in self-healing concrete, with particular focus on tubular encapsulation of healing agent, which are closely related to vascular healing systems. Other mechanisms for self-healing in concrete and vascular healing systems in other materials are then explored, before the scope of this project is defined at the end of the section.

2.1 Background and Key Definitions

Self-healing cementitious materials are not a new concept. Roman mortar is known to exhibit self-healing properties due to dry binder within the mortar spontaneously reacting with moisture in the air, closing microcracks in the material [8,9]. Whilst the mortar does not have particularly good global structural properties by modern standards, many large-scale Roman structures remained standing with little or no maintenance for nearly 2000 years before being weakened by the more aggressive post-industrial atmosphere. Whilst these mortars are not practical for modern day use, the exceptional longevity of structures built with them demonstrates the potential of self-healing to greatly increase the durability of concrete.

Recently, several international collaborative efforts have been made to consistently define self-healing cementitious material terminology [2,3,7,10,11].

2.1.1 Damage Prevention and Damage Management

Material failure is governed by bonds between atoms. Brittle materials such as unreinforced concrete are not able to stabilise damage from an initial crack and thus fail by fast fracture. Traditional material design has focussed on *prevention* of damage. That is, delaying the onset of an initial crack for as long as possible and attempting to slow any further damage. As these cracks remain in the material after loads are removed, the level of damage will always remain constant or increase, without external intervention (repair).

Self-healing materials introduce the concept of automatic damage *management*. The formation of damage is not deemed problematic as long as there is a subsequent corrective process [7].

The conceptual leap from damage management to self-healing materials lies in the level of automation of the repair process.

2.1.2 Autogenic and Autonomic Self-Healing

RILEM (The International Union of Laboratories and Experts in Construction Materials, Systems and Structures) has built on the work of the Japan Concrete Institute (JCI) [12] to define self-healing as 'any process by the material itself involving the recovery and hence improvement of a performance after an earlier action that had reduced [its] performance' [2]. This performance recovery can be divided into several overlapping mechanisms, summarised in the Venn diagram in figure 2.

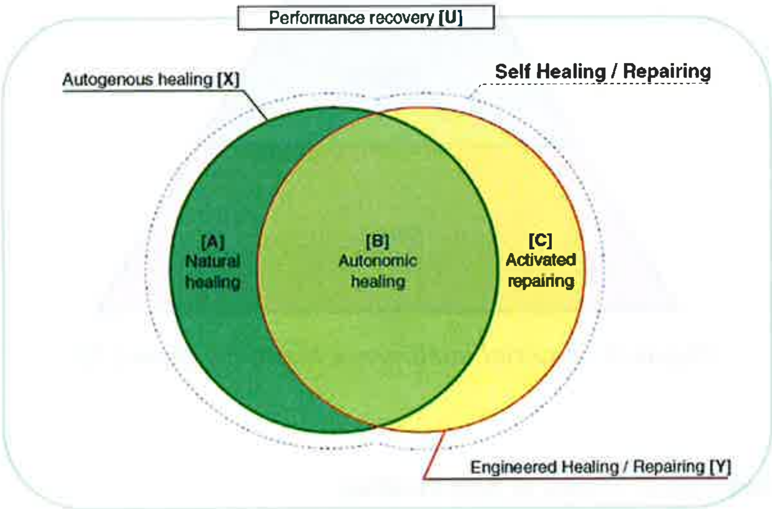

Figure 2: *JCI definitions of performance recovery subsets (from [12]).*

The key distinction identified by the RILEM technical committee in the case of self-healing concrete was that between auto*genic* (natural) and auto*nomic* healing, both of which are subsets of *autogenous* healing as defined by the JCI Venn diagram. Autogenic healing makes use of components of the material which are already present and not specifically designed for self-healing; autonomic healing uses engineered additives which would not otherwise be present in the material [2]. This project is specifically concerned with engineered additives (tubes, networks and healing agent), and thus falls into the autonomic healing category.

2.1.3 Basic, Smart and Intelligent Materials

The intelligence of materials can be categorised hierarchically (see figure 3). Most materials are "basic". Their response to external stimuli is purely a function of their mechanical properties. "Smart" materials 'provide a unique beneficial response when a particular change occurs in [their] surrounding environment' [13]. However, their response is normally an approximately linear function of a stimulus. "Intelligent" materials take this one step further by incorporating some control mechanism into their response. Generally, intelligent materials can gather, combine and process information to produce a controlled response to a stimulus. Many biological materials exhibit these properties [2].

Most self-healing materials fall into the category of smart *structures*: combinations of basic elements which exhibit some level of material intelligence when combined in an engineered way [3]. They are deemed smart rather than intelligent because the healing mechanism generally relies on some knowledge of how the damage is likely to occur.

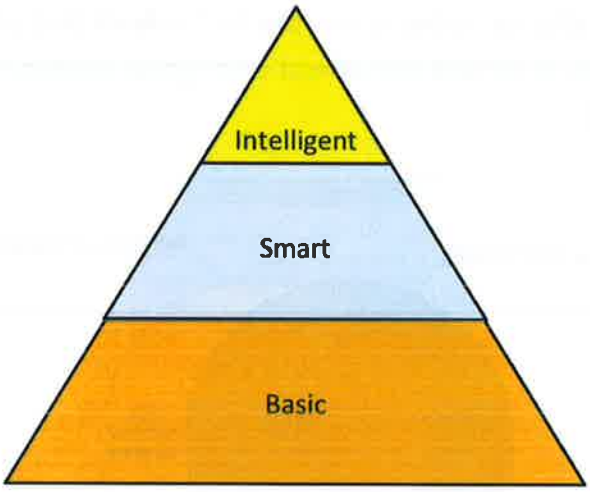

Figure 3: *Material intelligence hierarchy (from [2]).*

2.1.4 Passive and Active Modes of Self-Healing

Self-healing structures can also be categorised by the level of human intervention required to initiate the self-healing mechanism. "Passive" self-healing modes are initiated automatically at the onset of damage, whereas "active mode" self-healing requires human input. Some systems incorporate passive signalling of damage to indicate that active human intervention is required.

2.2 Desired Attributes of Self-Healing Materials

In their chapter on concrete in the book *Self Healing Materials* [14], Li and Yang identify a framework of 6 key attributes for ideal self-healing materials against which robust self-healing can be assessed:

1. **Pervasiveness**: the healing mechanism should be ready for local activation at any time;
2. **Stability**: it must remain active throughout the structure's design life (which may be much longer than conventional non-healing structures);
3. **Economics**: the solution must be financially viable as the construction industry is very sensitive to cost ;

4. **Reliability**: healing must occur in a wide range of environments with a very low failure rate;

5. **Quality**: the mechanical properties should recover to pre-damage levels or better;

6. **Repeatability**: it should be possible to heal multiple damage events.

The rest of this section will explore the extent to which these attributes have been achieved in other research and where there are opportunities for improvement.

2.3 Self-Healing in Cementitious Materials

The first major experimental work on self-healing in cementitious materials was performed almost exclusively by Carolyn Dry throughout the 1990s [15–21]. However, it was not until the release of a seminal paper on the autonomic healing of polymer composites in *Nature* by Scott White *et al.* that self-healing materials came to the full attention of the scientific community [22]. When White's paper was published in 2001, approximately 10 papers on self-healing materials were being published per year across the world; ten years later that figure had risen to 240 [23].

Van-Tittelboom [23] classified cementitious self-healing methods into three groups, drawing parallels from self-healing polymer research:

- **intrinsic, or autogenic healing**, in which the composition of the cementitious matrix is optimised to improve its natural self-healing mechanisms or other materials are added to the concrete mix to make an engineered cementitious composite (ECC);

- **capsule based healing**, in which static microcapsules containing a liquid healing agent are incorporated into the mix and designed to rupture as a crack propagates through the material;

- **vascular healing**, in which a network of hollow tubes connect the interior of the structure to a reservoir containing a liquid healing agent, which is released when the network is broken by a propagating crack.

Intrinsic healing has two major disadvantages. Firstly, the crack width must be restricted for the self-healing to be reliable. Depending on the environmental conditions and composition of the improved autogenous mix, different maximum allowable crack widths of 10-300 μm have been defined in various reports [14]. This highlights the other problem with improved autogenic healing: its low reliability and sensitivity to factors outside of the control of the designer. However, for specific applications, the low cost and effort of incorporating more additives into a concrete mix could make this method feasible.

Autonomic capsule based and vascular healing methods aim to reduce these issues associated with autogenic methods. In deciding whether capsule based or vascular healing is more suited to a particular application, a number of further considerations need to be examined. Capsule based systems are easier to incorporate at the mixing stage, although in larger concrete specimens they have been found to be unable to survive the casting process reliably. Also, once a given capsule's healing agent has been released, there is no way of replenishing it, leaving a void in the material, which will further reduce its strength. Vascular systems can be replenished and the probability of a crack intersecting a tube is higher than the probability of a crack intersecting a capsule, showing promise for multiple healing events. However, more consideration must be made regarding the network's scale, method of fabrication and practical issues, such as how to hold it in place and prevent ingress of concrete into the network during casting.

2.4 Biomimetic Vascular Networks

Vascular networks allow autonomic repair of multiple damage events in a particular structural region. This is important because stress concentrations in concrete members are normally localised. However, since concrete cracking is a brittle failure mechanism, the crack will originate at the weakest point in the vicinity of the largest tensile stresses so the exact location of fracture cannot be predicted accurately. Even if the initial crack is fully healed, the tensile stresses will remain, so further cracks can form around flaws in the same local region. The dynamic delivery of healing agent to where it is most needed means that vascular healing systems offer a distinct advantage over their capsule based counterparts, which cannot be replenished once the healing agent in a structural region has been expended.

The term "biomimetic" is often used to describe vascular networks because they are inherently inspired by natural phenomena. Natural intelligent materials almost always contain a tubular array which delivers some functional fluid through the material matrix, whether for molecular transport, signal propagation or waste disposal. They occur at a wide range of organised, hierarchical length scales and are often fractal in nature [24].

Care must be taken when drawing inspiration from natural materials, as the function designers try to mimic will often be grouped with several others for efficiency. For example, the vascular nature of animal circulatory systems serves the purpose of delivering clotting platelet cells to ruptured vessels, but must also carry gases, nutrients, hormones and waste products, antibodies to monitor for pathogens and white blood cells to fight disease, on top of regulating heat, pH and water content in every cell in the body. It would be foolish to blindly copy this level of complexity without considering which functions engineered self-healing materials require [25]. A considerably simpler solution may be sufficient for a vascular network which only serves the function of delivering a healing agent to a damage site, without the need for such precision of delivery location.

2.4.1 Early Work on Tubular Encapsulation in Concrete

In the early '90s, Dry experimented with different mechanisms to release adhesive from hollow porous fibres into cement matrices [15, 16], with the aim of reducing cracking, and consequently corrosion of reinforcement. By testing both active and passive modes of healing agent release, she was able to improve both the tensile and compressive strength of her samples and reduce their water permeability.

In the passive mode tests, small reinforced cement beams containing 16 glass capillary tubes filled with a single-component, air-curing adhesive were cast and then loaded in three-point bending. The results were compared to controls from a second set of tests, on samples with glass tubes containing no adhesive. The increase in load was stopped when the glass pipettes were heard to have broken. The samples were then left to heal for 14 days before being tested to failure. A representative diagram of the experimental set-up is shown in figure 4(a) and the results of the experiments are shown in figure 4(b).

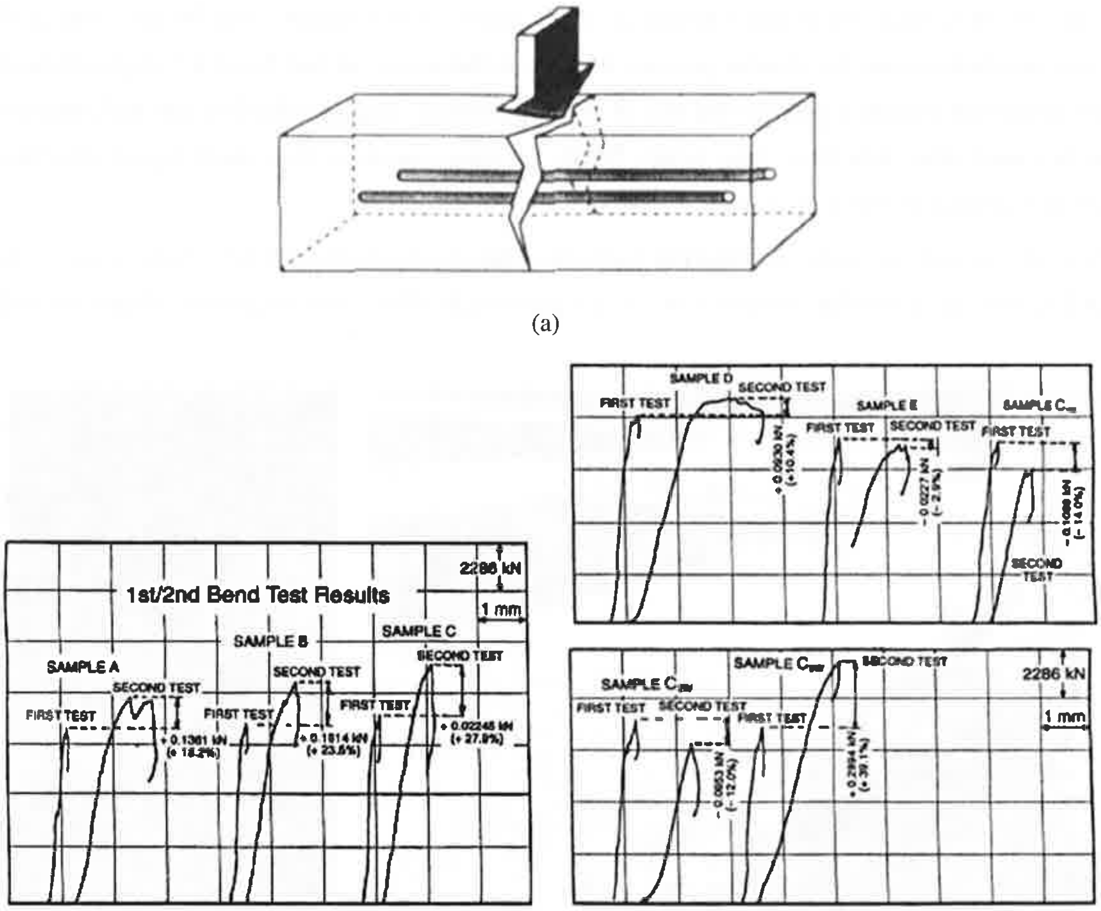

(a)

(b)

Figure 4: *Experimental setup and results from Carolyn Dry's 1994 paper [16]. (a) Load-displacement results from three-point bend test. (b) Timed release of chemicals occurs when the brittle fibre breaks under load.*

In general, the samples containing healing agent were found to increase in strength by approximately 15% on average, compared to a 4% increase in the control samples. Additionally, the healed samples exhibited increased toughness, shown by their ductility close to the failure load.

Dry followed her work up with investigations on beams containing hollow tunnels coated with brittle sealer, and filled with separated components of a three-part methyl methacrylate adhesive system [18]. It was found that the healed specimens exhibited greater proportional restored strength and flexibility than unhealed controls. However, the *absolute* strength values were not much improved after the healing cycle because the repaired beams had significantly lower initial strengths, due to the deletion of stiffer cementitious material in the healing tube's location.

By 1997, Dry had scaled her work up to real-size bridge deck slabs to study self-healing of cracks caused by shrinkage and internal shear [20, 21, 26]. Hollow glass fibres were scored to induce stress concentrations and cast into the surface of 4×20 ft bridge deck slabs to form a tubular network for the delivery of healing agent to cracked areas (see figure 5). The slabs were each tested three times in upward bending. They were several months old by the time of the first test and left in situ for similar periods of time in between, so had been left exposed to the environment for around a year by the end of the experiment. Liquid adhesive was still observed to be released after this time (see figure 5(b)), refuting concerns that such repair chemicals would not display stable longevity.

Visual assessment confirmed that the fully embedded tubes had cracked, whereas uncovered tubes had not, and partially covered tubes tended to break after a longer period of time than the

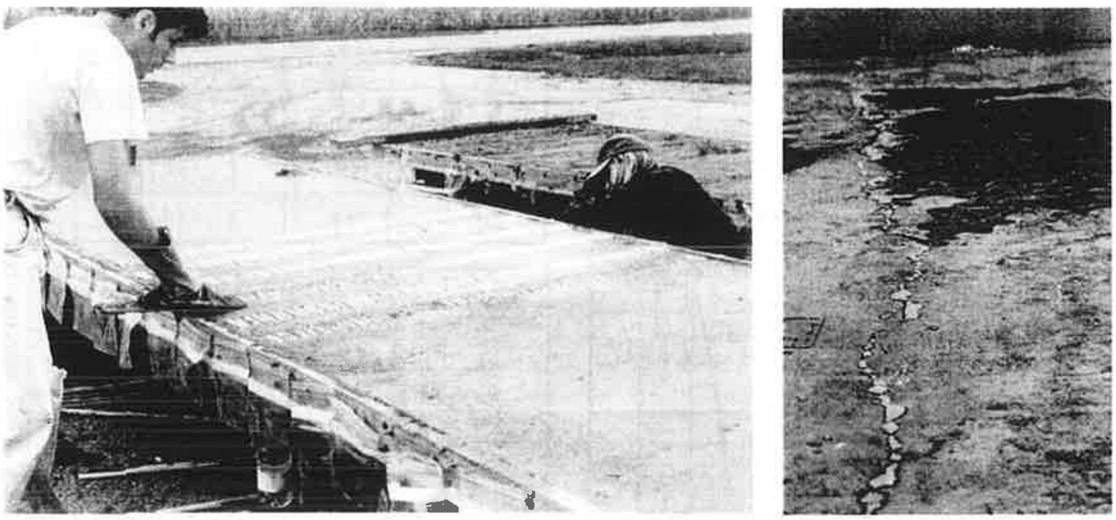

(a) (b)

Figure 5: *Dry's larger scale work combined embedded tubes into a vascular network. (a) Photograph of the tubes embedded into the top surface of the deck and (b) photograph of adhesive migrating into a crack as the slab is bent upwards (from [21]).*

fully embedded ones. Since the uncovered tubes were more exposed to harsh environmental conditions than the covered ones, Dry concluded that the tubes must have been fractured by shrinkage stresses rather than weather-related freeze-thaw cycles.

2.4.2 More Recent Studies

A number of research teams have followed on from where Dry left off since the turn of the century, and they have each taken a slightly different direction.

Epoxy resin was used as an air-curing healing agent by Tran Diep Phuoc Thao *et al.*, who performed similar tests to Dry on mortar specimens containing glass tubes [27]. The specimens were broken in three-point bending and left for 4 days, then broken again on day 7. It was found that the specimens' overall elastic modulus was reduced compared to control beam's as a result of the healing assembly having a lower stiffness than the deleted concrete. The second (day 4) loading cycle showed cracks forming at a lower load than the first cycle, but the third (day 7) loading cycle exhibited a 32% increase in strength on the virgin specimen (see figure 6(a)).

The location and nature of the formed cracks, shown in figure 6(b), were used to explain these results. As epoxy resin requires air to cure, it was suspected that the initial crack had only healed around the crack mouth, with the resin at the crack tip still in liquid form because of lack of air ingress at such small length scales. The second crack was initiated at a different location then merged with the first, opening another air channel to the epoxy. As the third crack did not merge with either the first or second crack, and the fracture strength had more than recovered, this would suggest that the second crack enabled full healing of the first, so the third was initiated at the next weakest point in the vicinity of greatest tensile stress.

Pang Sze Dai *et al.* extended these studies to larger concrete structural elements: 125 mm × 200 mm × 2 m beams, 200 mm Ø × 0.8 m columns and 100 mm × 1 m × 1 m slabs [28]. The glass tubes were encased in a 3.5 mm thick mortar layer to prevent damage, and premature release of healing agent, during casting. After repeated loading and unloading (three-point bending for the beams, compression for the columns and dropped weight impact for the slabs), the healing efficiency was assessed by stiffness recovery. The beams recovered up to 84%

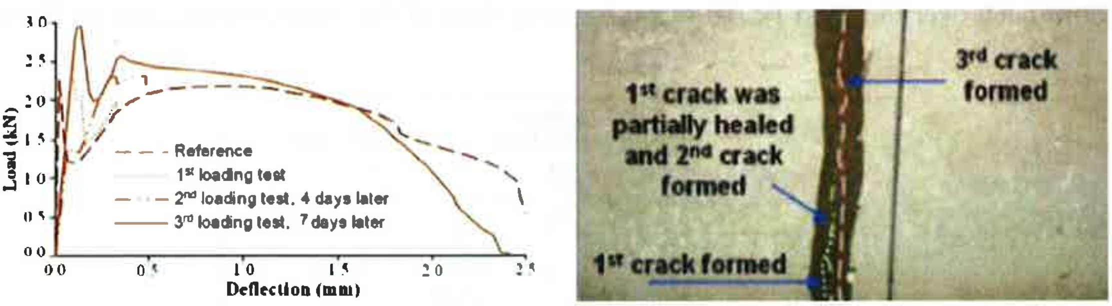

(a) (b)

Figure 6: *Key results from the investigations of Thao et al. (a) Load-deflection at 3-point bend application and (b) highlighted cracks and their order of formation.*

stiffness, the columns up to 70% and the slabs up to 99%. Because the crack planes in the column were horizontal, it was concluded that gravitational effects are not necessary for self-healing as capillary forces dominate.

Work on a numerical model for the autonomic self-healing process in concrete has been begun by Chris Joseph *et al.*, who mimicked Dry's work with the aim of extending the lattice beam modelling method to make predictions about healing efficacy [29,30]. They identified the major driving forces acting on an encapsulated healing agent (see figure 7) and intended to measure as many quantitative and qualitative parameters as possible (width, nature and location of cracks, adhesive properties, adhesive migration, strength and stiffness before and after healing, and strength and stiffness recovery), in order to gather a large amount of data for numerical modelling of the healing mechanism. A 5 centipoise (cPs) "wicking grade" cyanoacrylate adhesive was chosen as the healing agent because of its ability to heal very narrow cracks. The particular brand chosen was also suitable for bonding a wide range of materials and had relatively high tensile strength (20 MPa).

Preliminary investigations revealed that fully sealed encapsulation techniques, such as that shown in figure 7, did not allow sufficient adhesive migration due to the large negative pressure forces exerted at the wax plugs. The researchers thus decided to attach curved supply tubes to one end of the capsule, equalising the end pressure to atmospheric and adding a hydrostatic head to the pressure inside the specimen. This aided migration when the tubes were broken. Four capillary tubes were cast in each notched reinforced mortar specimen and the beams were loaded in three-point bending at a rate of 0.2 mm/min, until adhesive leakage was observed on the bottom face of the beam. The beams were then unloaded, left to heal for 24 hours and reloaded to failure. Typical results are shown in figure 8.

The results show that significant strength recovery was achieved along with extension of the linear-elastic region, and a slight increase in stiffness, after healing. A quality which had not been observed in other studies is "primary" healing, shown by the difference in load-carrying strength between the unhealed and control beams (up to around 25%). The authors concluded that this primary healing was the result of the low viscosity cyanoacrylate leaking into microcracks around the damage site. Because of the slow loading rate, these microcracks do not deform much over the short (< 10 second) curing time of the cyanoacrylate, and are healed

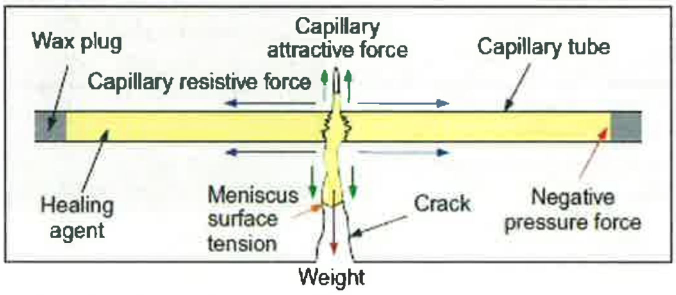

Figure 7: *The main forces acting on a sealed encapsulated healing agent (from [30]).*

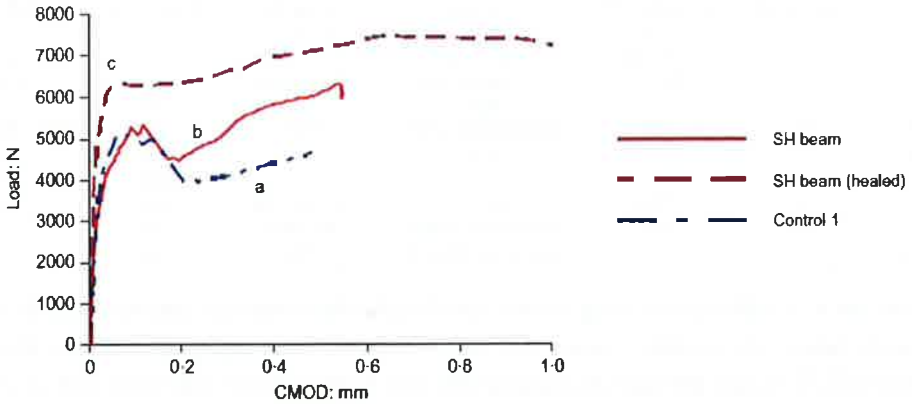

Figure 8: *Load vs Crack Mouth Opening Displacement (CMOD) plots for self-healing mortar beams and controls from Joseph et al.'s three-point bending experiments [30].*

almost as soon as the agent penetrates them. Further evidence for this behaviour is in the enhancement of strength and stiffness shown by "secondary" healing; it is believed that the region around the crack becomes a concrete-polymer composite with better material properties than either in isolation. As with the work of Thao *et al.*, the crack due to failure of the healed concrete did not intersect with the original crack, suggesting that full healing had occurred.

2.4.3 Healing Agent Requirements

In another paper, Joseph [3] identified four major requirements for adhesive healing agents on top of being abundant, available and economical. Agents for autonomic vascular self-healing should:

1. be suitable for internal encapsulation and stable until release;
2. be mobile between tube breakage and external damage locations;
3. have suitable mechanical properties for strength and stiffness recovery, enough toughness to resist repeat cracking and durability for the long term;
4. be compatible with the surrounding cementitious material.

A number of candidates exhibiting these properties to varying degree have been used in tests throughout the literature. Van Tittelboom combined his own conclusions on the properties of different healing agents [31] with those used by other researchers [23]. The findings for polymer adhesive agents are summarised in table 1:

Agent	Components	Viscosity [cPs]	Curing	Curing time	Expansion	Strength [MPa]
CA	1	<10	moist	seconds	no	20
EP1	1	250-500	moist, air, heat	60 °C, <100 min	no	22-25
EP2	2	80-360	component contact	30-60 min	no	5-45
MMA1	1	—	heat	—	no	—
MMA3	3	34	contact component	1 hr	no	50
Silicone	1	—	air	—	no	—
Foam	1	—	—	—	yes	—
PU1	1	7200	moist	40-180 min	yes	—
PU2	2	600	contact component	50-300 s	yes	—
Polyacrylate	2	7	contact component	40 s	no	—

Table 1: *Properties of different healing agents used in the literature as summarised by van Tittelboom. The wide ranges in parameters are a result of reports from different sources; the full table can be found in [23]. Gaps are due to parameters not having been reported. CA = cyanoacrylate, EP = epoxy resin, MMA = methyl methacrylate, PU = polyurethane.*

There is some disagreement over the optimal properties of these healing agents. Dry recommended 100-500 cPs viscosity on the basis of the American Concrete Institute (ACI) *Guide for the Selection of Polymer Adhesives with Concrete*, the rationale being that thinner healing agents are likely to flow out of a crack before curing, unless they are significantly thixotropic (shear-thinning) [17]. As noted earlier, Joseph *et al.* observed successful self-healing with 5 cPs fast-curing cyanoacrylate, which evidently does not suffer from the problem of leakage before curing [30].

2.5 Vascular Healing in Other Fields

Microvascular networks can be classified as either discrete channel arrays or interconnected networks [32]. Discrete channel arrays (like the tubular encapsulation techniques explored in earlier sections) show promise for autonomic self-healing in polymers, but suffer the same disadvantages: it is difficult to replace fluid to the depleted channel and the need for pervasive vasculature to heal damage in any location involves a trade-off between tube density and material properties. Interconnected networks somewhat reduce these issues, but the assembly of such networks is considerably more complex, particularly in three-dimensional geometries.

Since White *et al.* unveiled their microcapsule system for autonomic self-healing in structural polymers [22], the field has developed considerably faster than for construction materials. Self-healing polymers and composites have applications in military aerospace and consequently more freedom to conduct blue-sky research is afforded from private-sector grants. Ian Bond's team at the University of Bristol incorporated hollow glass fibres containing resin and hardener into bundles of e-glass fibres for self-healing in fibre-reinforced polymers (FRPs) for aircraft, reporting strength recovery up to 100% (although the initial strength of the self-healing composite was 16% less than the conventional FRP) [33,34]. White identified the future direction of the method as moving towards embedding "a circulatory system that continuously transports the necessary ... building blocks of healing to the site of damage" into the polymer matrix. By the end of the decade, Kathleen Toohey (of the same laboratory) had achieved this with one- [35] and two-part [36] healing agents (see figure 9), making use of direct-write assembly methods.

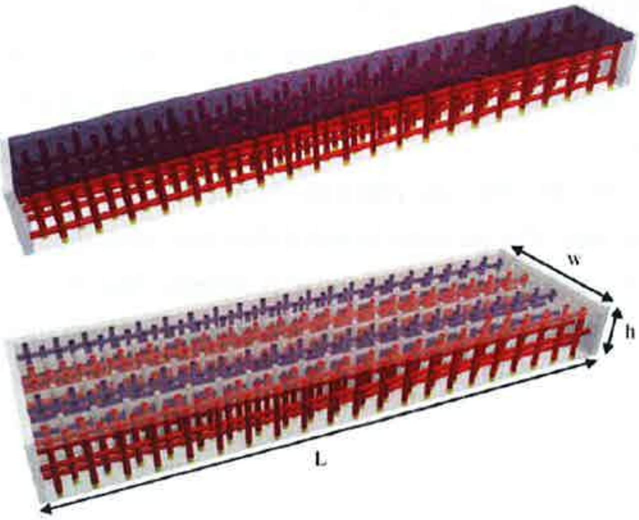

Figure 9: *Orthogonal microvascular network schematics for delivery of one- (top) and two-part (bottom) healing agents. In the two-part specimen, the different coloured networks do not intersect in order to keep the resin and curing agent separate (from [36]).*

Direct-write assembly involves the controlled extrusion of a viscoelastic ink, which can be robotically assembled into complex geometries on a layer-by-layer basis [37–39]. The inks are designed to be "fugitive" — after a material is cast around them they can be liquefied and removed by suction, leaving behind an interconnected network. Toohey's networks showed significant advantages over discrete channel arrays, particularly in their ability to heal multiple occurrences of damage (the one-part healing agent could heal up to 7 consecutive damage events in a single sample and the two-part agent could heal up to 16).

2.6 This Project

This project aimed to build on the research detailed above by linking the research on self-healing in cementitious materials with the interconnected microvascular networks utilised in self-healing polymers. Because mortar contains sand particles which are large compared to the millimetre-scale microfluidic networks offered by direct-writing of fugitive inks, it was anticipated that direct analogy with this approach would prove unfeasible. Instead it was envisaged that larger-scale interconnected networks would be designed.

The literature review revealed several issues that needed consideration when designing these networks for use in concrete.

Firstly, if an air curing agent is used, there must be a reliable route for air ingress into the crack. Due to the narrow channel width at a crack's tip, the crack itself may not be sufficient for this air transport.

Secondly, the networks must be tough enough to withstand the casting process, but brittle enough to break as soon after the concrete cracks as possible, so careful consideration of network material properties would be required.

Thirdly, the construction of interconnected vascular networks is not trivial. Neither is the installation process — how the networks are held in place while a thick material matrix is cast around it without gaps.

Vascular networks are flexible and efficient, mimicking the mechanisms that nature has evolved to heal its materials. The potential rewards that they offer the self-healing process more than justify the effort expended to solve the above problems. The rest of this report details how the issues were tackled and tested, and discusses the extent to which they were solved.

3 Apparatus and Methodology

3.1 Apparatus

3.1.1 Casting Apparatus

Three-point bending of small square prismatic specimens was adopted as the primary testing procedure, in keeping with the experiments of Dry and Joseph described in section 2. Mortar was chosen as the cementitious material because large aggregates would be incompatible with the small mould size, particularly when crowded with networks and reinforcement in later tests. High strength (52.5) Ordinary Portland Cement (PC) was used in the mortar composition, along with sand with a maximum particle size of approximately 2 mm and tap water. After some experimentation, the mix adopted was 0.55:1:3 (water : cement : sand by weight), which was fluid enough to fill small gaps between components in the moulds without causing over-hydration problems.

The preliminary tests were conducted in 40 mm × 40 mm × 160 mm prismatic moulds, with later tests moved into 50 mm × 50 mm × 225 mm moulds for two reasons. Firstly, the larger cross-sectional area allowed more space for multiple tubes to pass through the cross section. Additionally, the larger moulds had interchangeable end-pieces, allowing circular notches to be drilled into wooden square sections for supporting the tubes and reducing the likelihood of concrete ingress which would cause blockages after curing.

For specimens in the larger moulds, single mild steel bars of 3 mm Ø circular cross-section were used for light tensile reinforcement, giving a reinforcement : concrete area ratio of 0.3%. The bars were bent 90° at the ends so that they were 180 mm long, leaving approximately 15 mm at each end for anchorage, and bonded to 7 mm thick ceramic spacers with silicone rubber bathroom filler. A typical set-up before pouring is shown in figure 10.

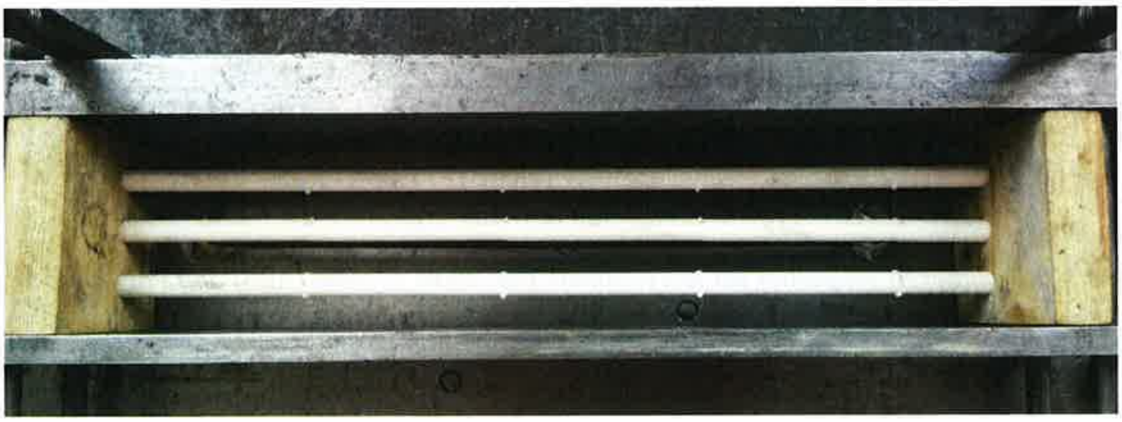

Figure 10: *50 mm × 50 mm × 225 mm mould prepared with three hollow PLA tubes of 6 mm outer diameter slotted into the end-pieces. The reinforcing steel bar on top of the ceramic spacers can be seen underneath the tubes.*

3.1.2 Network Construction Apparatus

Tubes and networks were constructed using three dimensional (3D) printing. 3D printing is an additive manufacturing technique used to robotically build parts from Computer Aided Designs (CAD), much like the direct ink writing techniques described in section 2.5. It requires very little tooling after production, and has the flexibility to create parts of almost any geometry. Vascular networks were built using a single head CubeX™ 3D printer, which can print in either Acrylonitrile Butadiene Styrene (ABS) or Polylactic Acid (PLA). A model of the desired object is designed and built on a computer (using software called Cubify® Invent™), and sliced along its z-axis by the compiling CubeX™ software. These sections are then used to instruct a print-head where to deposit layers of fixed thickness on the horizontal (x-y) plane, in much the same way as a conventional inkjet printer deposits ink on paper. The print bed is then moved down the z-axis by the same distance as the layer thickness, and the next layer is deposited on top. This process is iterated until the part is finished (see figure 11).

Figure 11: *Progression of the 3D printing process. The final output is shown in figure 19(b).*

The maximum dimensions for a part printed using the single head CubeX™ model are 275 mm (x) × 265 mm (y) × 240 mm (z), with tolerances of ± 1% in the x- and y-directions [40]. The computer models can be segmented in the z-direction into layers of 100 µm, 250 µm or 500 µm thickness. Some bulk material properties of the ABS and PLA [41] are compared in table 2.

	ABS	**PLA**
Young's Modulus (GPa)	1.9	3.5
Ultimate Tensile Strength (MPa)	40	50
Density (g/cm^3)	1.06	1.25
Typical Elongation at Break	20%	6%

Table 2: *Key material properties for Acrylonitrile Butadiene Styrene (ABS) and Polylactic Acid (PLA), the two print materials available for the CubeX™ [41].*

Because of its higher stiffness and lower strain at failure than ABS, it was deduced that PLA would be more compatible with cementitious materials, which typically form cracks at relatively small displacements due to their weakness in tension. However, as will be explained later, it was suspected that the directional details of the 3D printing process would lead to these materials having considerably different properties as printed parts than they do in bulk.

3.1.3 Testing Apparatus

The three-point bend tests were performed in an Instron® 5967 Dual Column Tabletop Universal Testing System, with a $\pm$ 30 kN load cell attached. Cement pastes with water : cement ratios of 1:1, 2:1 and 3:1 were used as healing agents, along with cyanoacrylate glues of low (3 cPs) [42] and high (100 cPs) [43] viscosity (technical details can be found in table 3). Blue tracer dye was used in control specimens to visualise fluid transport after cracking.

Glue Type	**Viscosity**	**Tensile Strength**	**Cure Time** (fully set)
Low Viscosity	1-3 cPs	up to 23 MPa	2-10 s (24 hr)
High Viscosity	100-120 cPs	28-32 MPa	up to 60 s

Table 3: *Properties of low and high viscosity cyanoacrylate adhesives used as healing agents. Full technical data can be found in [42] and [43].*

Crack width and healing agent pervasion were measured optically, using image processing software ImageJ [44]. By placing a ruler in the photograph frame in the plane of the surface to be analysed, the software can be calibrated to millimetres per pixel, and used to measure distances and areas by counting pixels enclosed by user-drawn shapes and converting to SI units.

3.2 Sample Preparation Procedure

3.2.1 Mould set-up

The moulds were prepared as described in section 3.1, with reinforcing bars and healing tubes aligned as required by the specifics of the test. The cement and sand were weighed and blended in a cement mixer for 1-2 minutes before half of the required water was added. After another 1-2 minutes of mixing, the rest of the water was added, and the mixer was left to run for another 2 minutes until a homogenous mixture had been achieved.

3.2.2 Casting

The mortar was poured into the moulds on a vibration table to remove air bubbles as it was poured. The vibration amplitude was set large enough that the moulds "rattled" rather than "buzzed", but not so large that they moved significantly around the table. The bubbles were removed from the top of the moulds and new wet mortar was added to the top until bubbles stopped forming on the surface after 5-10 minutes.

3.2.3 Curing

After 24 hours, the samples were labelled and carefully removed from the moulds and submerged in water for curing for 7 days. They were then removed from the water bath and left to dry for a further 24 hours before being tested.

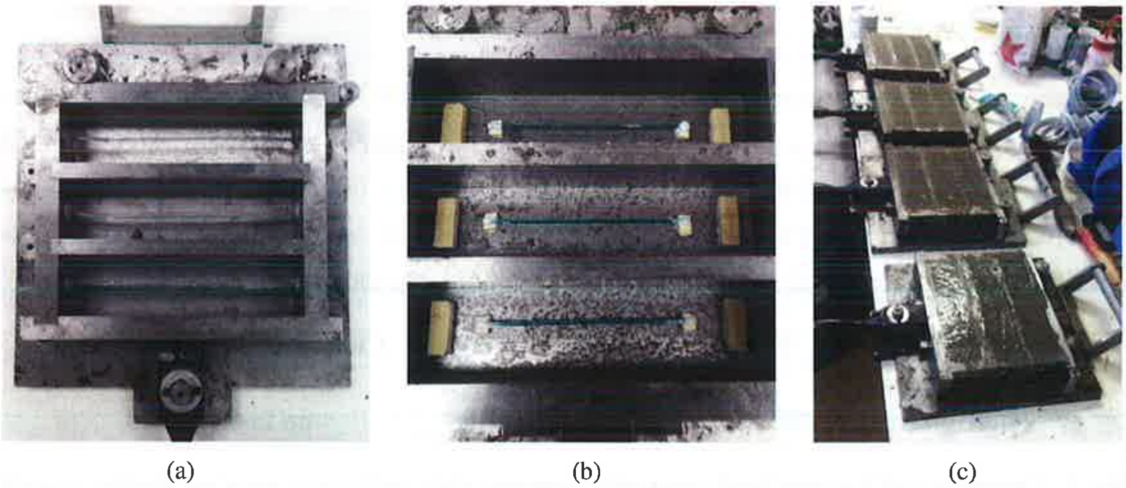

Figure 12: *Preliminary experimental set-up. (a) Flexible tubing was fed through pre-made holes in the ends of the mould to connect the dye-filled pipette to the atmosphere; (b) sealed pipettes were mounted on ceramic spacers stuck to the bottom of the mould and (c) the cast samples drying in the lab.*

3.3 Experimental Methods

3.3.1 Preliminary Investigations

Preliminary tests were carried out on unreinforced mortar specimens, cast in the 40 mm × 40 mm × 160 mm moulds, containing 1 mm Ø glass pipettes filled with tracer dye. Samples with pipettes connected to the atmosphere by flexible tubing from a peristaltic pump (figure 12(a)) were compared to samples with pipettes sealed at the ends with silicone rubber bathroom filler (figure 12(b)).

All samples were loaded to the point of first cracking at a rate of 0.05 mm/min in three-point bending and the crack faces analysed qualitatively. It was found that the tubes did not break reliably at the same time or location as the mortar, and also that those which did crack demonstrated limited leaking efficacy. As might be expected, the leakage was significantly better in those tubes which were open to the atmosphere than in the tubes with sealed ends; the dye pervaded to a roughly circular diameter approximately 3 times larger than the outer diameter of the pipette in the open-ended specimens (see figure 13(a)), whilst there was no noticeable leakage in the closed-ended specimens. This area was quantified using ImageJ and observed to be around 6% of the total.

As is typical in brittle fracture, it is difficult to control the location of cracking without prior notching of the material — failure occurs wherever the largest natural defect is in a region of large stress. The chances of both the mortar and glass failing in the same plane is thus very low, and many tube cracks were over 10 mm away from the sample crack plane. In these cases, it was possible to see that only around 2 mm^3 had leaked even from the open tubes (see figure 13(b)). Holding the tubes vertically did not cause the fluid to flow out either. This suggests that pressure

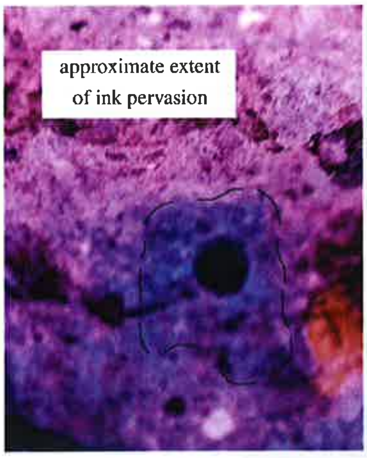

(a)

(b)

Figure 13: *Typical crack faces from preliminary experiments. (a) Ink is predominantly transported by capillary action, to a maximum distance of approximately twice the diameter of the pipette and (b) further evidence for capillary transport shown by the small volume of dye which leaked from the cracked tube.*

forces at the open end are insufficient to overcome viscous forces inside such a small tube, and the only fluid that did leak was drawn out by capillary action. It was thus decided that future tubes and networks would be constructed with significantly wider internal diameter: above 3 mm.

3.3.2 Free Tubular Members

After some experimentation printing simple tubes, it was found that the only suitable print orientation for producing networks which break easily was to align the tube axis with the z-axis of the printer (i.e. extrude the tubes vertically). Because the layers are aligned in parallel planes, 3D printed parts have anisotropic material properties. In particular, the joints between adjacent layers do not carry tension well, so are susceptible to brittle fracture in bending if they are aligned perpendicular to the tensile bending stress (see figure 14).

Because the print head imposes horizontal loads on the top of a printed part when depositing the next layer, large tensile reactions can occur at the base of slender designs, which may dislodge them from the print bed and cause the print to fail (figure 15(a)). To reduce this effect and save time, tubes and networks were printed in batches, rigidly connected at various points along their length to reduce the resultant moment at the base (figure 15(b)).

A tensile reaction force T occurs at the points labelled A in figure 15. Taking moments about point B, which experiences a non-critical compressive force of equal magnitude, on the slender tube in figure 15(a) gives

$$T_{slender} = \frac{FL - mgr}{2r}, \tag{1}$$

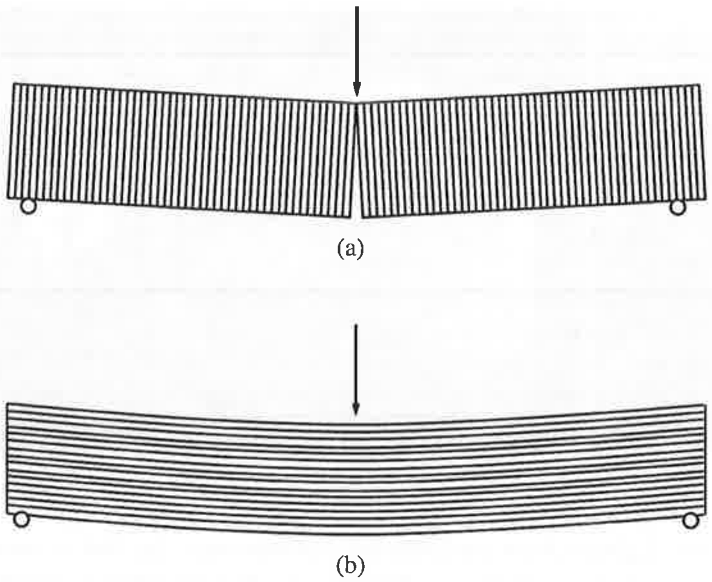

Figure 14: *The material properties of 3D printed parts are anisotropic, much like a unidirectional fibre composite material. (a) When bending stresses induced by the load act perpendicular to the print plane, the tube behaves in a brittle fashion because the joints between deposited layers do not carry tension well. (b) When bending stresses induced by the load act parallel to the print plane, the tube behaves elastically because the joints are carrying much smaller shear stresses as individual layers are bending.*

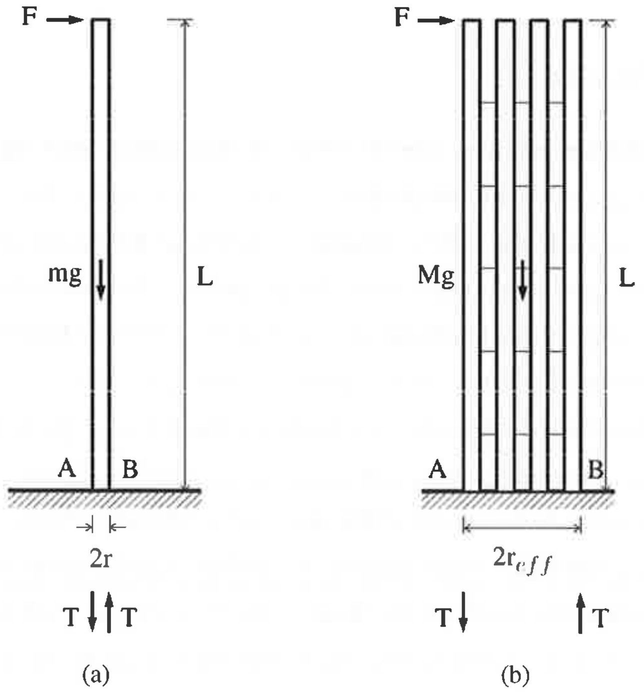

Figure 15: *The forces acting on (a) a single slender tubular member and (b) an interconnected array of tubular members as the print head moves over the top of the part to deposit a new layer.*

where T is the tensile reaction force, F is the force from the print head, mg is the weight of the printed part, r is its half-width and L is its length.

Taking moments about point B on the less slender coupled tubes gives

$$T_{connected} = \frac{FL - Mgr_{eff}}{2r_{eff}}, \tag{2}$$

where $M > m$ and $r_{eff} > r$. Increasing the number of tubes printed at once therefore improves the structural integrity of the part whilst printing by reducing the tensile stresses on the base. Whilst this proved the only effective way of printing tubes in their brittle orientation, it did result in large imperfections along the tubes' length when they were cut away which affected their fracture behaviour (visible in figure 16(b)).

Bearing in mind the qualitative findings of these preliminary tests, tubular sections of various sizes and layer thicknesses were printed and loaded to failure in three-point bending, while the imposed central displacement and resulting load were recorded. The aim of these tests was to determine which tube geometries would be most compatible with the surrounding mortar and to gain a qualitative understanding of how they might fracture when embedded. It was envisaged that the results would allow quantification of the anisotropic material properties of the tubes in their brittle orientation to allow comparison with the bulk properties of PLA. In particular, it was hoped that there would be an optimum trade-off between wide internal diameter (to maximise the Reynolds number of the flow) and narrow external diameter (to minimise the reduction in strength and stiffness of the specimen due to deletion of concrete). Considering these requirements, whatever the optimum diameter of the tube, its wall thickness should be as thin as is practically feasible. CAD models were therefore built of negligible wall thickness, to force the CubeX™ to print the tube walls with the minimum thickness it is capable of. The nominal and actual dimensions of the tested tubes are detailed in the appendix, but they will be referred to by their nominal diameter (ND, dimensions in mm) from here.

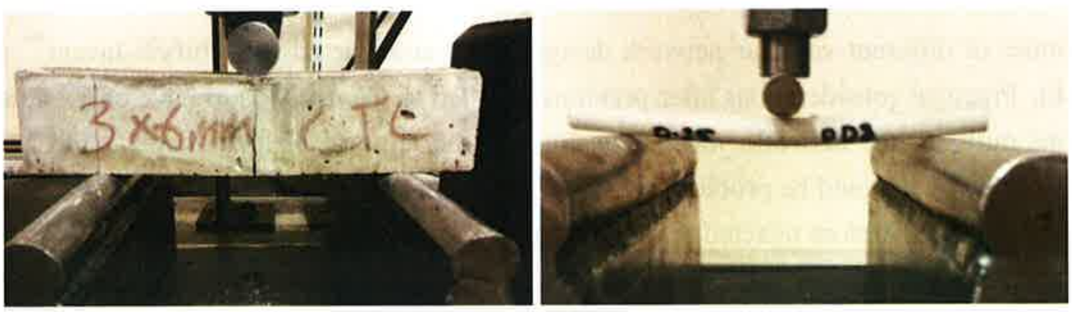

(a) (b)

Figure 16: *Three-point bending in the Instron® Universal Testing System. (a) Typical mortar specimen and (b) 3D printed tube, showing support imperfections on the compressive side.*

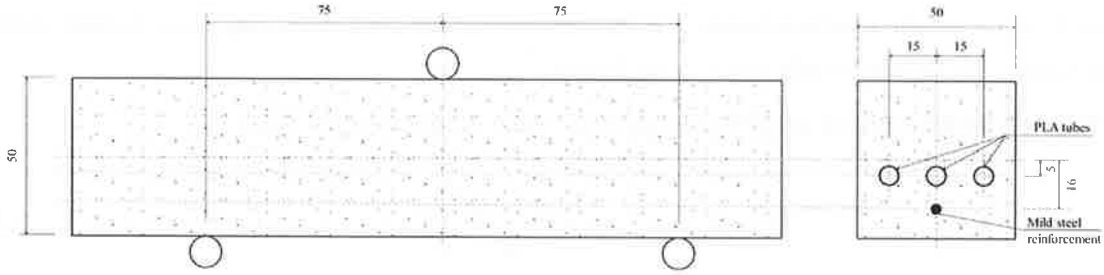

Figure 17: *Specimen side and end views for three-point bend testing. All dimensions in mm.*

3.3.3 Embedded Tubes

Three-point bend tests were performed on 50 mm × 50 mm × 225 mm lightly reinforced mortar specimens with ND10, ND8, ND6 and ND5 tubes embedded in them, after flow tests on the ND4 and ND3.5 tubes showed that their internal diameters were too small for viscous healing agents. 5 beam types were cast: 5 with one ND10 tube embedded, 5 with one ND6 tube, 5 with one ND5, 5 with three ND6 tubes distributed horizontally, and 5 with three ND5 tubes. Cement pastes of 3:1, 2:1 and 1:1 water : cement ratios were tested alongside the high viscosity cyanoacrylate adhesive and a tracer dye, used as a control, in each of the 6 beam types. The typical layout is shown in figure 17.

The samples were loaded to the point of first cracking, at which point the test was stopped. Then, the healing agent was injected along the length of the tube using a syringe. The loading was started again until audible cracking of the tube was heard and subsequent reduction in carried load was observed. The syringe was then pressurised until leakage of healing agent was observed at the crack face, when the test was stopped.

The samples were then left for a week to heal; a week being chosen to allow the cement pastes time to recover strength. They were then reloaded in three-point bending until failure and subsequently fractured completely to allow visual analysis of the crack plane.

3.3.4 Vascular Networks

A number of different vascular network designs were constructed in Cubify® Invent™ (figure 18). Practical considerations after previous tests led to the decision to have only one inlet and one outlet to the network; more than this and the removal of air bubbles could not be guaranteed, which would be problematic for air curing healing agents. The complex design in figure 18(b) was therefore rejected despite being the most directly biomimetic solution.

Another consideration which must be taken when designing 3D printed parts is their verticality. Elevated horizontal members such as arch structures cannot be printed because there is nothing to lay the print material on without including structural support in the design. It was desired to keep the network design as vertical as possible, both to minimise the amount of material wasted on structural support to be cut away and to maximise the brittle fracture effect described in section 3.3.2. For this reason, the orthogonal design based on Toohey's networks

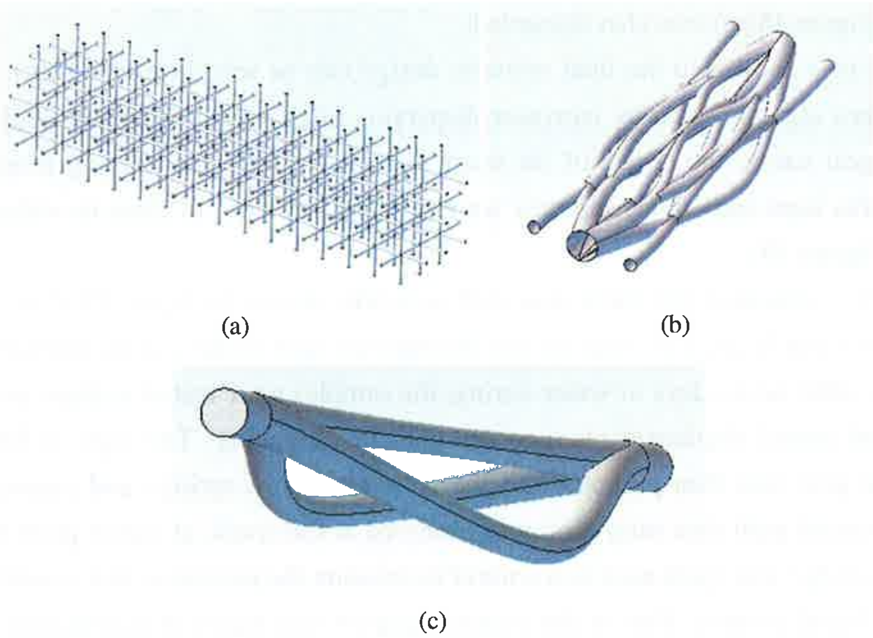

Figure 18: *Model concept designs for vascular healing networks. (a) An interconnected orthogonal array in three dimensions; (b) a complex vascular design mimicking blood vessels and (c) a simple design for dispersing tubes at the region of largest stress.*

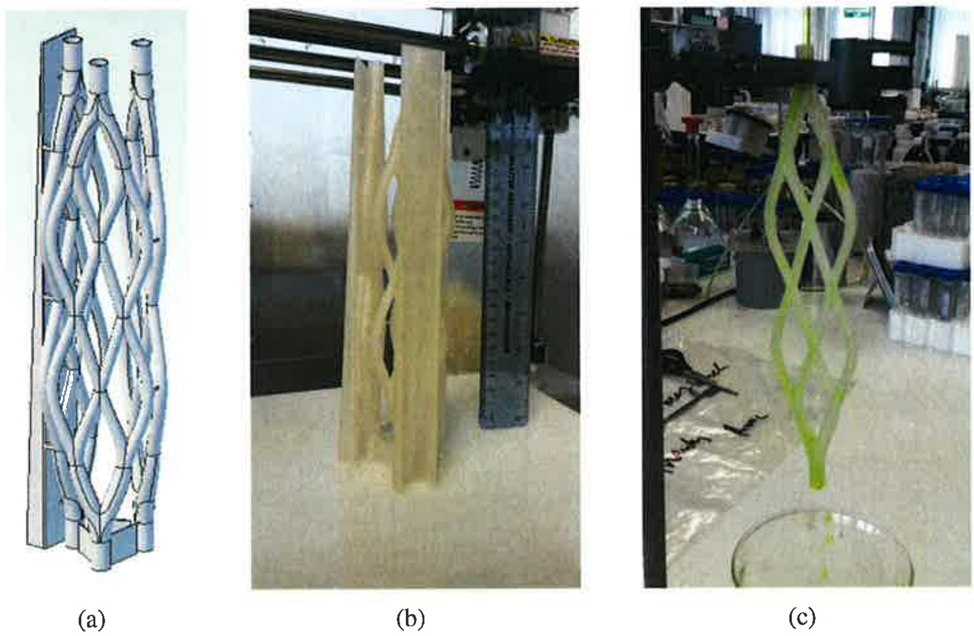

Figure 19: *The networks used in testing. Three networks were printed at once to save time and improve structural stability during printing. (a) The model designed in Cubify® Invent™ (with two of the three supports cut away for clarity); (b) the output of the 3D printer and (c) an individual network after the supports had been cut away demonstrating flow with no blockages or leaks.*

in polymers (figure 18(a)) was also discarded.

The principles applied to the final network design can be seen in figure 18(c). Wide inlet and outlet tubes are connected by narrower dispersing tubes which distribute fluid around the region of largest stress; the centre of the beam's span. To keep the printing process simple, planar networks were settled on, and they were printed in batches of three to widen their base for stability (figure 19).

10 samples containing the interconnected networks shown in figure 19(c) were cast (although one was lost because the seal around the network inlet broke and the network was filled with mortar). After seven days of water-curing, the samples were tested in three-point bending with loads and central displacements recorded until first cracking. The high- or low-viscosity cyanoacrylate glue was then pumped into the network with a syringe and pressurised. The load was increased until glue migration was observed at the crack, at which point the test was stopped. Tracer dye was again used as a control to measure the pervasion that would be possible with a 1 cPs liquid (water). One of the control samples was tested in asymmetric three-point bending to check that the network would break in any crack plane. The samples were then retested to failure after either 24 or 48 hours.

4 Results and Discussion

4.1 Free Tubular Members

The free tubes exhibited fairly ideal linear-elastic brittle behaviour, with the carried load increasing proportionally to the central displacement imposed by the testing machine until sudden catastrophic failure. The loads and displacements at failure can be found in the appendix along with details on the location of the crack and the geometry of the tubes tested.

All tubes were observed to crack along the connections between printed layers. However, stress concentrations at the imperfections where the tubes had been connected together for printing meant that the fracture location was normally far from the applied load. This behaviour was not observed when the tubes were embedded, suggesting that the mortar imposes compatibility constraints on the tubes which force them to crack at the same location as the surrounding material.

The bending stiffnesses and Young's moduli are shown in figure 20. Since

$$\delta = \frac{WL^3}{48EI} \tag{3}$$

for a simply supported beam with a central point load [45], the bending stiffness load is given by

$$EI = \frac{WL^3}{48\delta} \tag{4}$$

where EI is the bending stiffness, W is the central load, L is the distance between supports and δ is the central displacement. The Young's modulus E is calculated by dividing the result by the 2$^{\text{nd}}$ moment of area I.

The second moment of area was calculated assuming that the tubes were perfect thick walled cylinders, which led to significant inaccuracies in the calculation of Young's modulus as shown by the wide spread in figure 20(b). In particular the large values of E for the tubes with layer thicknesses of 0.1 mm are due to the print head starting and finishing at the same point each time it laid down a circle, which caused increased wall thickness on one side of the tube; a problem which was more acute for the 0.1 mm layer thickness tubes. A layer thickness of 0.25 mm was chosen as standard for the remaining tests because of its balance between good resolution in the z-direction and precision in the x- and y-directions.

These data show that the Young's modulus of extruded tubes printed in PLA is significantly higher than it is for PLA in bulk. This means that stresses in the material will be larger for a given applied strain, increasing the tubes' compatibility with stiff, low strain-to-failure concrete. Combined with the sudden brittle fracture property of tubes printed in this way, these tubes are ideal for encapsulating healing agent within concrete. They are also not as fragile as glass pipettes, which may mean that the casting process is less likely to cause damage, even in larger members.

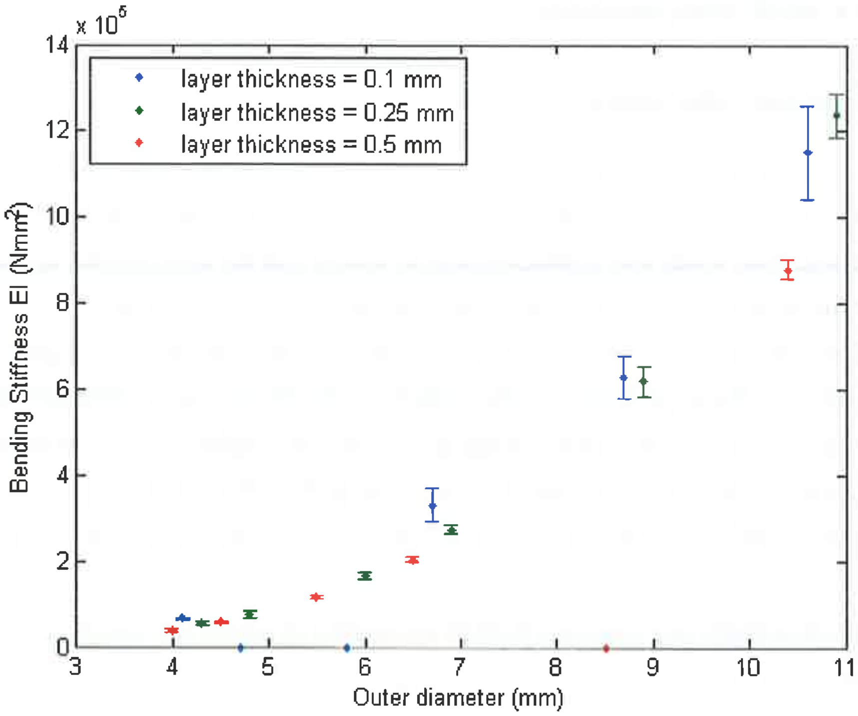

(a)

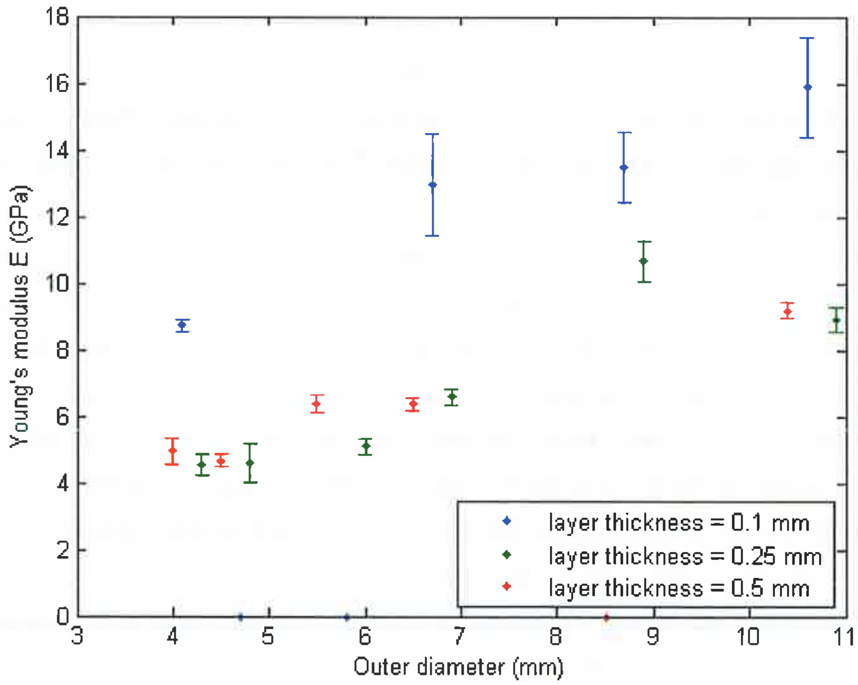

(b)

Figure 20: *Data obtained from three point bend tests on free 3D printed tubular members. (a) Measured bending stiffnesses and (b) calculated Young's moduli.*

4.2 Embedded Tubes

Healing Agent	Tube Layout	Strength Recovery	Stiffness Recovery	Crack Width (µm)
1) 1:1 cement paste	1×10	36.5%	56.0%	1110
	1×6	23.5%	62.5%	230
	1×5	—	—	—
	3×6	84.0%	37.0%	1060
	3×5	—	—	—
2) 2:1 cement paste	1×10	46.5%	50.5%	220
	1×6	60.5%	33.5%	550
	1×5	43.5%	32.0%	670
	3×6	64.0%	39.5%	490
	3×5	104.5%	56.0%	450
3) 3:1 cement paste	1×10	30.5%	25.0%	380
	1×6	—	—	—
	1×5	43.5%	41.5%	380
	3×6	54.0%	35.5%	310
	3×5	75.0%	49.0%	380
4) 100 cPs cyanoacrylate	1×10	56.0%	40.5%	1020
	1×6	79.5%	55.0%	990
	1×5	94.0%	43.5%	930
	3×6	80.0%	57.5%	1040
	3×5	—	—	—
5) Tracer dye (control)	1×10	31.0%	26.0%	500
	1×6	44.0%	37.0%	590
	1×5	42.5%	33.5%	510
	3×6	59.5%	41.5%	690
	3×5	52.0%	39.0%	790

Table 4: *Strength and stiffness recovery proportions for specimens with embedded tubes and the crack widths at first leakage. The load-displacement plots can be found in the appendix. Some results are missing as the healing agent did not leak either because the tube was blocked in the casting process or the internal diameter was too small.*

Table 4 shows the recoveries in strength and stiffness of specimens tested with embedded tubes. Because the beams contained reinforcement, all recoveries must be compared to the control specimens (set 5, filled with tracer dye). Although some self-healing may be expected after pumping water through a tight crack, it was not expected that the effect would be significant in this case as cracks were widened to over 500 µm before leakage was observed in the majority of cases.

The best self-healing was effected in a specimen with three ND5 tubes containing 2:1 cement paste; the only specimen to show strength recovery above pre-damage levels. The cement paste generally filled the cracks well, as demonstrated in figure 21, but generally, little stiffness recovery was observed in comparison to controls.

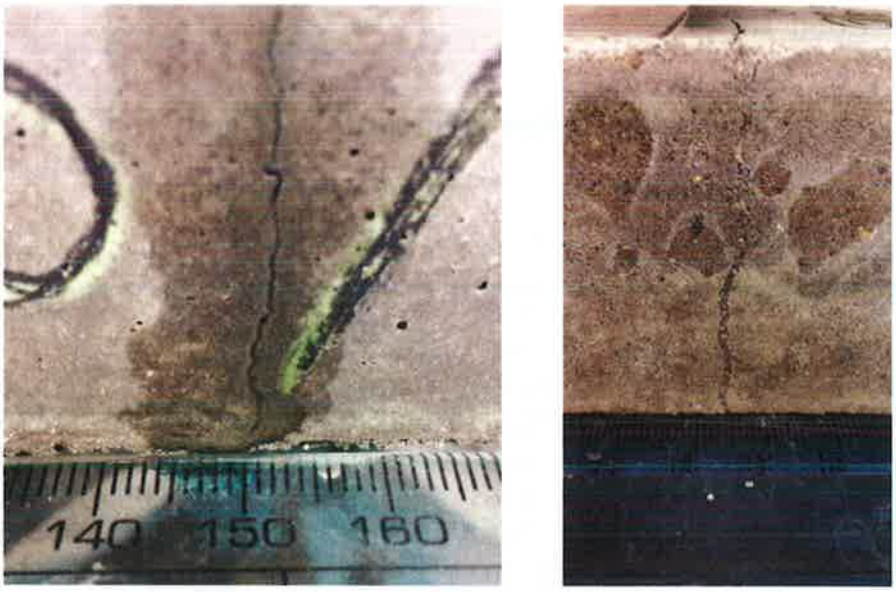

(a) (b)

Figure 21: *Cement paste was observed to leak into cracks. (a) The wet paste leaking during the first test and (b) the dried paste had sealed the crack by the second test.*

Consistent strength recovery was observed when the cyanoacrylate was used as a healing agent, with all but one of the specimens showing strength recovery of around 80% or more. The ND10 tube cracked, but very little leakage was observed as can be seen in figure 22(a). Much better strength recovery was observed when the glue migrated throughout the crack face (figures 22(b) and 22(c)), as expected.

The stiffness recovery was generally bad, showing little improvement on the controls with the exception of some outliers. These outliers generally leaked at lower crack widths. Whilst it is not possible to draw conclusions about causation from such a small amount of data, it seems intuitive that larger crack widths, for which the reinforcement has likely exceeded its elastic limit (and in some cases its ultimate tensile strength), will be unable to demonstrate the same stiffness recovery as small crack widths, when the reinforcement has not yielded. Particularly the viscous cyanoacrylate was difficult to force to leak, even with high pressurisation from a syringe. This is reflected in the large crack widths at leakage observed (see figure 23).

Because of the promising strength recovery observed when using viscous cyanoacrylate as a healing agent, it was decided to test its performance against ultra-low viscosity "wicking grade" cyanoacrylate in the final tests on specimens with embedded microvascular networks. Whilst the good self-sealing properties of cement paste were noted, the best seals were achieved by the pastes with the highest water content because they were most fluid, but these pastes also displayed the worst strength and stiffness recovery in general, so were discarded for further testing to reduce the number of networks it was required to print. It was suspected that lower viscosity cyanoacrylate would fill cracks more reliably than the 100 cPs variety, and also maintain its significant strength recovery.

(a) (b) (c)

Figure 22: *Somewhat counter-intuitively, the viscous glue migrated further from narrow tubes than it did from wider ones. (a) Only around 6.5% of the total concrete area was reached by the glue from the 10 mm Ø tube. (b) A large improvement is seen with the 6 mm Ø tube, and (c) three 6 mm Ø tubes facilitated 80% crack face coverage.*

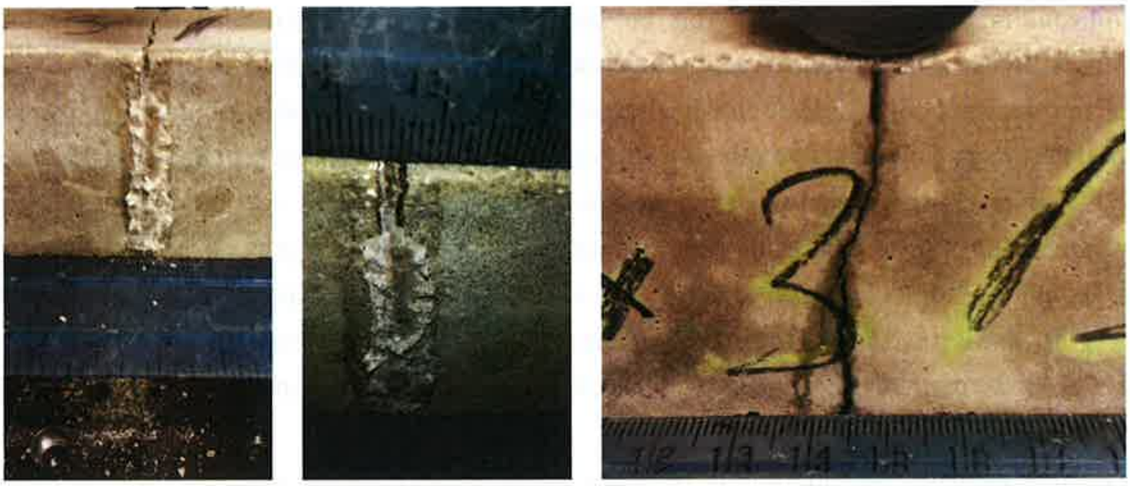

(a) (b) (c)

Figure 23: *Particularly for the more viscous 1:1 cement paste and cyanoacrylate, the required crack width for leakage was inhibitively large for effective self-healing. Leakage was not observed for some specimens with embedded tubes until the crack width was as large as 1000 μm.*

4.3 Vascular Networks

The strength and stiffness recoveries for specimens with embedded vascular networks are shown in table 5. All samples were retested after 24 hours, except for 6 and 9 which were left for 48 hours before being retested. A further control specimen (number 5) was tested in an off-centre three-point bend. The results are not included in table 5 because they are not consistent with the mechanism used to test other specimens. The network was observed to crack in the same location as the concrete, approximately 50 mm from the centre of the beam, and the tracer dye

Healing Agent and Identifier	**Strength Recovery**	**Stiffness Recovery**	**Crack Width** (μm)
Control 1	42.0%	13.5%	130
Control 2	43.0%	50.0%	140
High viscosity 3	52.5%	69.0%	210
High viscosity 7	51.5%	76.5%	190
High viscosity 6*	71.5%	70.0%	190
Low viscosity 8	42.0%	74.0%	140
Low viscosity 10	59.5%	81.5%	160
Low viscosity 9*	65.0%	99.5%	150

Table 5: *Strength and stiffness recovery proportions for specimens with embedded vascular networks filled with high and low viscosity cyanoacrylates and the crack widths at first leakage. The load-displacement plots can be found in the appendix. *Samples 6 and 9 were retested after 48 hours, the rest after 24 hours.*

leaked out effectively, covering 100% of the crack plane.

The embedded network specimens show a significant improvement in stiffness recovery over the embedded tubes and compared to the controls. The strength recovery is not reliably a significant improvement on the controls, but there is evidence for improvement over the second 24 hours. Because both cyanoacrylates are quoted to be fully cured within 24 hours, this points to a contribution from autogenic self-healing within the concrete — curing of unreacted cement within the crack. This is more likely to be the case for these vascularised specimens as the crack width is so much tighter, and would suggest that the glue's strength is not sufficient to heal the specimens fully. Since both cyanoacrylates have quoted tensile strengths of over 20 MPa (table 3), which is high compared to the tensile strength of concrete (typically 2-6 MPa [46]), if this is the case it is a result of the porous nature of concrete making it unsuitable for good bonding with these particular cyanoacrylates which are designed for non-porous metals, ceramics and polymers.

Further evidence for glue failure is shown by the location of the new crack. In all cases, the second failure occurred in the same location as the first (figure 24). This could be predicted by the results — if the new crack formed anywhere other than the original crack, the regained strength and stiffness would have to be close to the original values. Because cracks propagate from at the weakest point in a state of high tensile stress, if the glue had bonded the crack planes perfectly a new crack would have formed.

The improved stiffness recovery seems most likely to be the result of the much lower crack width at leakage. Clearly, the required crack width for leakage from vascular networks is much smaller than it is for leakage from simple tubes. Qualitatively, leakage was also achieved with far less pressure exerted on the syringe used to fill the network than the discrete tubes. The "high viscosity" cyanoacrylate used in this set of tests is the same as the 100 cPs glue used in section 4.2. In the embedded tube tests, the average crack width for leaking was 1 mm, whereas the average for embedded networks was 200 μm — a reduction of 80%. The required crack

Figure 24: *Little evidence was seen of new crack plane formation; the new crack is within the porous region that the low viscosity glue has filled.*

widths for lower viscosity cyanoacrylate and water-based tracer dye were even lower: 150 μm and 140 μm respectively. Typical photographs of this leakage are shown in figure 25.

There are two likely causes for this earlier leakage: cracking of the network occurring closer to the cracking of the concrete and reduction in resistive forces within the network. As can be seen on the load-displacement plots in the appendix, the second sharp drop in the curve (indicating fracture of the plastic) generally occurs closer to the first sharp drop (indicating fracture of the concrete) in the networks than in the tubes. Consequently, the additional displacement required to open the plastic crack wide enough for leakage results in a smaller overall crack width at leakage. This consistently earlier plastic cracking has something to do with the shape of the networks compared to the single tubes. Because the connected networks are wider, they are stiffer in bending, and thus the same imposed strain will result in a larger peak stress, in turn leading to brittle fracture at a smaller central displacement, and therefore crack width. However, it can also be observed from the plots in the appendix that the loading did not need to be continued for as long after the cracking of the plastic for leakage to be observed either, so the resistive forces exerted by the network on the fluid must also be reduced.

The geometry of the networks used in this study (they contain loops, see figure 19(c) from section 3.3.4) means that internal circulation of fluid is possible without external pressure. If one

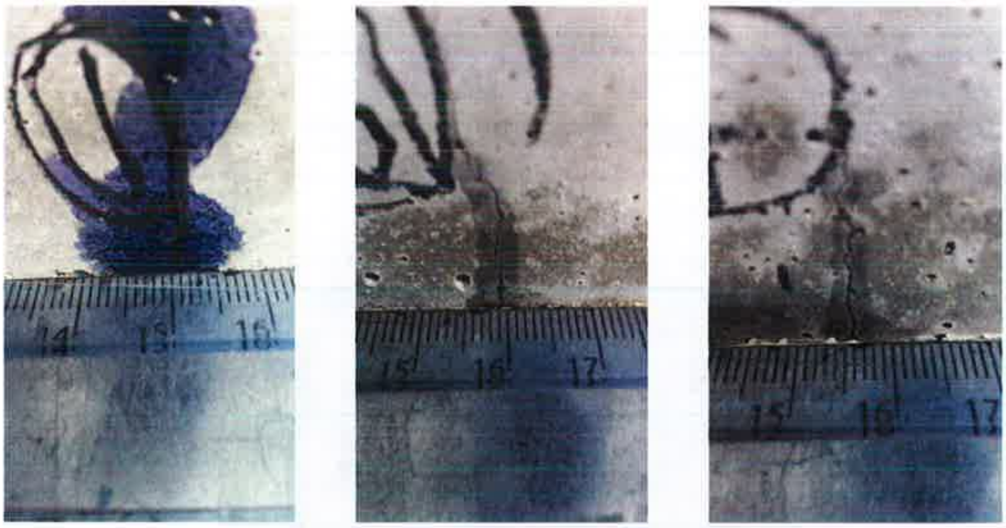

(a) (b) (c)

Figure 25: *The required crack widths for fluid leakage were far lower for embedded vascular networks, even with viscous healing agent. (a) The tracer dye used as a control leaked with a crack width of under 150 μm, (b) low viscosity cyanoacrylate leaked through cracks of around 150 μm and (c) higher viscosity cyanoacrylate leaked through 200 μm cracks.*

of the loops is broken, as occurs anywhere in-between the two primary forks, a new single tube open to the atmosphere at both ends is effectively formed. Because this loop is far shorter than the distance between the inlet and outlet of a long tube, the viscous friction forces do not have as much distance to act over, and so the length scale of the problem is reduced (in fluid mechanics terminology, the Reynolds number is increased; viscous forces become less important relative to inertial forces). This reduces the overall resistive forces and facilitates earlier release of healing agent. Another consequence of internal circulation in the loops is that it is difficult to remove air bubbles, which reduce the average viscosity in the tube and consequently also the resistive forces.

Another improvement that vascular healing systems show is in the migration of the healing agent. In contrast to the embedded tube tests, in general the coverage was comprehensive. The worst pervasion (62%) was observed in the high viscosity cyanoacrylate specimens and the best in the low viscosity cyanoacrylate specimens (85%). The tracer dye used as a control migrated across the entire crack face (figure 26). This enhanced transport is another result of the reduction in resistive forces that facilitate earlier leakage.

Finally, it should be noted that when the specimens were retested 24 or 48 hours after the cyanoacrylate was injected, it was not possible to cause further flow in the network because it had been blocked by the glue which had solidified in the crack. This could have been caused by air ingress into the crack or bubbles in the tubular network. The solidification of healing agent after one activation represents a major limitation to the practicality of this set-up for applications beyond the laboratory, although some solutions not already attempted in the literature are presented in section 5.3.

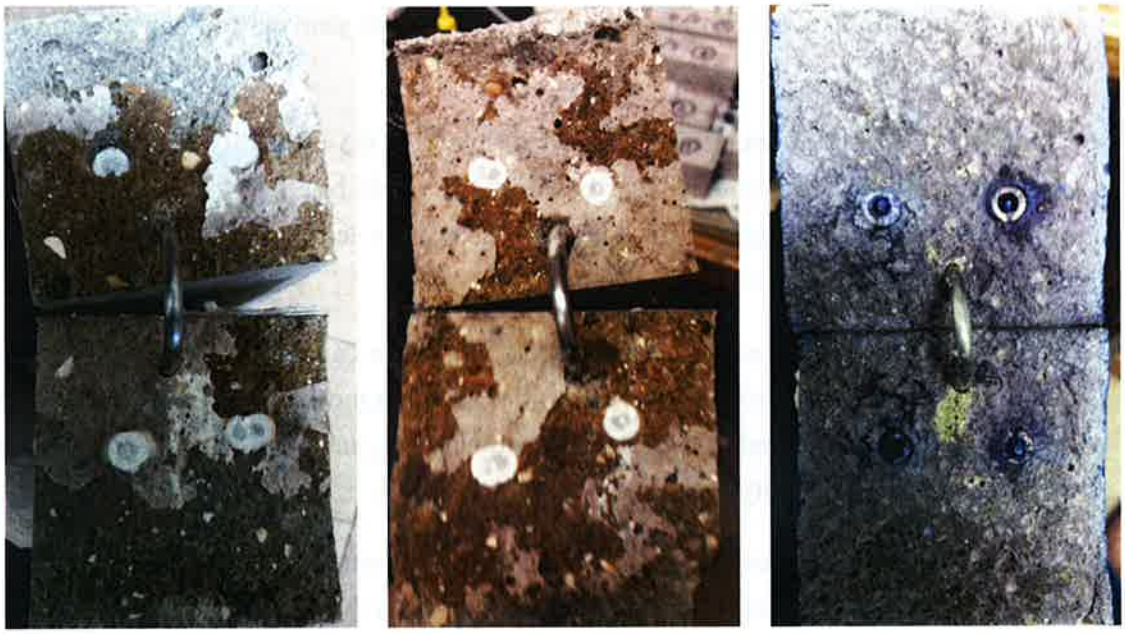

(a) (b) (c)

Figure 26: *Migration was also more reliable with embedded vascular networks. (a) The worst coverage was 62% with high viscosity cyanoacrylate, (b) the best coverage was 85% from low viscosity cyanoacrylate, and (c) the tracer dye reached 100% of the crack face. These findings suggest the healing agent should be as low viscosity as possible to minimise the required network density.*

4.4 Summary

3D printed vascular networks show some promise for use as self-healing systems in cementitious materials. They can be assessed against the "Desired Attributes of Self-Healing Materials" framework detailed in section 2.2:

1. **Pervasiveness**: the crack plane coverage with healing agent ranged from 62% to 85%, with controls reaching 100%. Coverage was demonstrated at a different location along the beam by the offset three-point bend test. Local activation was therefore demonstrated, and was effective at any time (within the short timescale of the experiment).

2. **Stability**: As noted above, the experiment timescale was very short compared to the design lifetime of a typical concrete structure. Whilst stability over a period of months has been demonstrated by Dry [21], stability over a period of years yet to be proven and represents a significant gap in the research literature.

3. **Economics**: Detailed analysis of the financial cost of these systems has not been performed, but its scalability is likely to be limited by the practicality of large-scale 3D printing in the present state of the technology. The additional workmanship required to build and insert vascular networks during cast at present need not be a barrier in the

future, as the installation is no more complex in principle than casting concrete around reinforcement.

4. **Reliability**: More tests would be required to quantify the reliability of healing. The interconnected vascular systems were certainly more reliable than the isolated tubular systems because of the tighter crack width required for leakage. A range of healing environments was not tested.

5. **Quality**: The mechanical properties did not recover to pre-damage levels. Further testing would be required to ascertain why this was the case, but most adhesives require contact pressure to effectively bond, which was not present here, and could have had a negative effect on the healing quality.

6. **Repeatability**: As noted earlier, this self-healing mechanism is not repeatable in its current configuration due to solidification of adhesive within the network.

Further work needs to be done to make biomimetic vascular networks for self-healing concrete a viable option over autogenic or microcapsule based healing. However, these results have proven a concept and suggested future directions for this research, which will be explored in the next section.

5 Conclusion

5.1 Key Findings

Sustainability has become an increasingly important issue in the construction industry. Self-healing concrete systems offer an opportunity to reduce cost and cement consumption in maintenance of civil engineering structures.

After gathering information on the state of the art in self-healing cementitious materials and vascular networks for healing, experimental work was guided by qualitative findings from preliminary tests. Notably, the internal diameter of any healing tube should be greater than 3 mm and mortar test specimens should be reinforced to allow controlled crack growth, otherwise healing agent will not leak.

The material properties of 3D printed plastics were found to be anisotropic due to the planar deposition of material in the printing process and non-uniform properties between layers. Tubes printed vertically behave like brittle materials, while horizontally printed tubes are much more ductile. Tests performed on vertically printed tubes showed that this property increases their bending stiffness and Young's modulus in comparison to the bulk material properties of the plastic.

Healing was unreliable, and stiffness recovery insignificant, in mortar specimens containing open tubes filled with healing agent because the crack width required for leakage was very large; sometimes over 1 mm.

The crack width at leakage was between 130 mm and 210 mm when interconnected networks were used as healing systems, and consequently the stiffness recovery was improved to between 70% and 100%, compared to a maximum of 50% in control specimens. Lower viscosity cyanoacrylate performed better than the higher viscosity cyanoacrylate in this regard, and both glues showed significant improvement in strength recovery when left to heal for a day longer than their quoted curing times.

It was postulated that the required crack width for leakage was smaller when networks were used for healing because of their looped geometry. When a loop is broken, the effective length of the healing tube, and therefore the magnitude of resistive viscous forces, is reduced. The networks also cracked at lower strains than the isolated tubes because they had a higher second moment of area. Consequently their bending stiffness was larger and smaller strains exerted larger tensile stresses.

5.2 Improvements

The major advantage of biomimetic vascular systems over discrete tubular arrays is their pervasiveness. Improved healing agent migration in the crack plane was achieved and activation by a crack in an arbitrary location was demonstrated.

Any improvements to the system should attempt to maintain these good qualities, whilst trying to improve on the limitations in reliability, repeatability and quality. A good area to explore first would be the repeatability of healing; this is a potential "showstopper". Without repeatability, vascular systems have no advantage, and significant disadvantages, compared to simpler microencapsulation techniques which have already shown progress in the self-healing of cementitious materials. Another essential future improvement is in the reliability quality of strength and stiffness recovery; they would ideally both be around or over 100%.

Extending the biomimetic analogy beyond the concept of a tubular delivery system, blockage would be less common if healing agent could be pumped through, either continuously or when required. Pumping before testing could remove air bubbles from the circuit and reduce the likelihood of curing within the network. If the healing agent was circulated immediately after cracking, the pump pressure could force adhesive into the gap *and* prevent curing across the break in the network.

Further studies would need to be undertaken to understand how biological vascular systems reseal themselves without being blocked after healing damage to the surrounding material. It is likely that a more complex damage sensor would be required to control when the fluid is pumped to reduce power consumption, upgrading the self-healing material from a smart structure to an intelligent structure.

5.3 Recommendations for Future Work

As demonstrated by the wide spread in results, and variety of shapes of load-displacement graph shown in the appendix, concrete testing is inherently uncertain. Any future work must therefore first attempt to obtain more data to reduce this uncertainty and obtain more reliable figures for strength and stiffness recovery.

Some future avenues for this research could be explored in a year. Others, drawing inspiration from the literature, would require more time. A few ideas for future investigations are detailed below.

Short term projects

- *Cast networks in larger members.* It would be interesting to see how well this method could be applied to more practical sized specimens such as those used by Pang *et al.* [28]. A larger specimen size would allow a more accurate optimisation of the distance between tubes: maximising coverage of the crack face by healing agent whilst minimising the volume fraction of concrete displaced by tubes. It would also clarify the volume of polymer and healing agent that would be required to make this technique feasible in the field.

- *Design 3D print sized modules.* The networks tested here were built to the maximum height of the 3D printer. Testing in larger members would require some method for connecting smaller vascular modules together to create a pervasive network. It may be possible to design the equivalent of a "plumber's toolkit" for building vascular networks from prefabricated parts. Connectors could also be designed in the 3D printer, or the thermosoftening plastic could be heated at the connection to join the pipes continuously.

- *Investigate other methods of circulating healing agent.* The peristaltic pump idea mentioned above is one possibility. Another would be to imitate "Tube a Manchette" systems for compensation grouting in tunnelling projects, as cement paste showed some promise as a healing agent.

- *Design systems which will heal other failure modes.* Tensile cracking is only one possible mode of failure of concrete structures. Shrinkage and shear cracking would not necessarily rupture the networks investigated here. The ideal self-healing vascular network would be able to heal damage without making prior assumptions about its type.

- *Use a crack-closure system to apply pressure to the crack face while healing.* Crack closure has been achieved in autogenic self-healing with some success [14]. These or simpler methods for forcing the crack face together could be all that is required to increase strength and stiffness recovery to above pre-damage levels.

Longer term projects

- *Model damage and healing.* Joseph analysed healing using lattice modelling methods [29] and Nguyen has undertaken progressive damage finite element analysis with regard to self-healing in composites [47]. If these and other models could be combined, it may be possible to describe the entire process mathematically, and make numerical predictions about how it could be improved.

- *Investigate new methods of visualising the healing process.* Most events of interest in concrete self-healing occur within the specimen and cannot be visualised conventionally. These events thus have to be inferred aurally or from behaviour on a load-displacement graph, which is less certain. Van Tittelboom investigated healing using computed tomography (CT) scanning [48]. Modified versions of other forms of medical imaging may be applicable to vascular self-healing such as Positron Emission Tomography (PET), Single Photon Emission Computed Tomography (SPECT) or Magnetic Resonance Imaging (MRI) may also be useful in visualising self-healing, particularly if they could do so in real time.

Concrete's wide use in construction means there are huge potential financial and sustainability gains to be made by developing a material which will last longer in service with less maintenance. Self-healing systems are a possible solution to the problem of cracking in brittle materials, and show potential for improving the durability of concrete.

Vascular systems for self-healing draw a direct parallel from biological systems, which almost all incorporate interconnected fractal networks for delivering functional fluids through the material. Some progress has been made in building such networks with a 3D printer. With further work in future years, it is hoped that improved strength and stiffness recovery will be demonstrated and a system will be developed which can heal itself on multiple occasions. In the longer term, these intelligent structures could come to dominate the built environment as much as concretes do now and render such unsustainable systems obsolete.

Acknowledgements

I would like to thank Dr Abir Al-Tabbaa for her supervision of the project, patience, knowledge of the literature and suggestions for experimental work.

Also invaluable were Dr Al-Tabbaa's research group. I'd particularly like to thank Dr Antonis Kanellopoulos for his guidance, encouragement, experimental experience and help with the 3D printer, and doctorate student Tanvir Qureshi for his help with experimental design and analysis of results. In addition, Division D technicians Chris Knight, Martin Touhey and Phil McLaren were extremely helpful throughout and I would like to thank them for sharing their expertise in practical matters.

References

[1] H.G. van Oss. Background facts and issues concerning cement and cement data. *Open-file report 2005-1152*, 2005.

[2] M. de Rooj, K. van Tittelboom, N. de Belie, and E. Schlangen (eds). Self-healing phenomena in cement-based materials. *Draft of State-of-the-Art report of RILEM Technical Committee*, 2013.

[3] E. Schlangen and C. Joseph. Self healing processes in concrete. *Self-healing materials: Fundamentals, design strategies, and applications (S.K. Ghosh, ed)*, 2009.

[4] J. Woodhuysen and I. Abley. *Why is construction so backward?* Wiley-Academy, 2004.

[5] K. van Beugel. Is there a market for self-healing cement-based materials? In *Proceedings of the First International Conference on Self-Healing Materials*. Noordwijk aan Zee, The Netherlands, 2007.

[6] J.M. Allwood, J.M. Cullen, M.A. Carruth, D.R. Cooper, M. McBrien, R.L. Milford, M.C. Moynihan, and A.C.H. Patel. *Sustainable materials: with both eyes open*. UIT Cambridge Limited, 2012.

[7] S. van der Zwaag (ed). Self healing materials: an alternative approach to 20 centuries of materials science. *Springer Series in Materials Science*, 100, 2007.

[8] M.P. Riccardi, P. Duminuco, C. Tomasi, and P. Ferloni. Thermal, microscopic and X-ray diffraction studies on some ancient mortars. *Thermochimica acta*, **321**(1): 207–214, 1998.

[9] P.F. Brune, A.I. Ingraffea, M.D. Jackson, and R. Perucchio. The toughness of Imperial Roman concrete. In *Proc. 7th Int. Conf. on Fracture Mechanics of Concrete and Concrete Structures*. Korea Concrete Institute, Seoul, 2012.

[10] E. Schlangen, H. Jonkers, S. Qian, and A. Garcia. Recent advances on self healing of concrete. In *Proceedings of Fracture Mechanics of Concrete and Concrete Structures: Recent Advances in Fracture Mechanics of Concrete (B.H. Oh* et al., *eds)*. Korea Concrete Institue, Seoul, 2010.

[11] M. Wu, B. Johannesson, and M. Geiker. A review: Self-healing in cementitious materials and engineered cementitious composite as a self-healing material. *Construction and Building Materials*, **28**(1): 571–583, 2012.

[12] S. Igarashi, M. Kunieda, and T. Nishiwaki. Research activity of JCI technical committee TC-075B: Autogenous healing in cementitious materials. In *Proceedings of 4th International Conference on Construction Materials: Performance, Innovations and Structural Implications, ConMat*, pages 89–96, 2009.

[13] S.R. Sharp and G.G. Clemena. State-of-the-art survey of advanced materials and their potential application in highway infrastructure. Technical report, 2004.

[14] V.C. Li and E. Yang. Self healing in concrete materials. In *Self healing materials*, pages 161–193. Springer, 2007.

[15] C.M. Dry. *Design of systems for time delayed activated internal release of chemicals in concrete from porous fibers, aggregates of prills, to improve durability*. PhD thesis, 1991.

[16] C. Dry. Matrix cracking repair and filling using active and passive modes for smart timed release of chemicals from fibers into cement matrices. *Smart Mater Struct*, **3**(2): 118–123, 1994.

[17] C.M. Dry. Smart multiphase composite materials that repair themselves by a release of liquids that become solids. In *1994 North American Conference on Smart Structures and Materials*, pages 62–70. International Society for Optics and Photonics, 1994.

[18] C. Dry and W. McMillan. Three-part methylmethacrylate adhesive system as an internal delivery system for smart responsive concrete. *Smart Mater Struct*, **5**(3): 297–300, 1996.

[19] C.M. Dry. Improvement in reinforcing bond strength in reinforced concrete with self repairing chemical adhesives. In *Smart Mater Struct*, pages 44–50. International Society for Optics and Photonics, May 1997.

[20] C.M. Dry. Release of smart chemicals for the in-service repair of bridges and roadways. In *Symposium on Smart Materials, Structures and MEMS*, pages 140–144. San Diego, California, 1998.

[21] C.M. Dry. Three designs for the internal release of sealants, adhesives, and waterproofing chemicals into concrete to reduce permeability. *Cement and Concrete Research*, **30**(12): 1969–1977, 2000.

[22] S.R. White, N.R. Sottos, P.H. Geubelle, J.S. Moore, M.R. Kessler, S.R. Sriram, E.N. Brown, and S. Viswanathan. Autonomic healing of polymer composites. *Nature*, **409**(6822): 794–797, 2001.

[23] K. Van Tittelboom and N. De Belie. Self-healing in cementitious materials—a review. *Materials*, **6**(6): 2182–2217, 2013.

[24] M. Nosonovsky and P.K. Rohatgi. *Biomimetics in Materials Science: Self-healing, self-lubricating, and self-cleaning materials*, volume 152. Springer, 2011.

[25] S. Van der Zwaag, N.H. Van Dijk, H.M. Jonkers, S.D. Mookhoek, and W.G. Sloof. Self-healing behaviour in man-made engineering materials: bioinspired but taking into account their intrinsic character. *Philos T Roy Soc A*, **367**(1894): 1689–1704, 2009.

[26] C.M. Dry. Repair and prevention of damage due to transverse shrinkage cracks in bridge decks. In *1999 Symposium on Smart Structures and Materials*, pages 253–256. International Society for Optics and Photonics, 1999.

[27] T.D.P. Thao, T.J.S. Johnson, Q.S. Tong, and P.S. Dai. Implementation of self-healing in concrete - proof of concept. *The IES Journal Part A: Civil & Structural Engineering*, **2**(2): 116–125, 2009.

[28] S.D. Pang, P.T. Tran Diep, and S.T. Quek. Self-healing concrete structural elements. In *3rd International Conference on Self-healing Materials (I. Bond & R. Varley, eds)*, pages 322–323. Bath, UK, 2011.

[29] C. Joseph and A.D. Jefferson. Stochastic regularisation of lattice modelling for the failure of quasi-brittle materials. *Proceedings of FRAMCOS6: Fracture Mechanics of Concrete and Concrete Structures*, pages 445–52, 2007.

[30] C. Joseph, A.D. Jefferson, B. Isaacs, R. Lark, and D. Gardner. Experimental investigation of adhesive-based self-healing of cementitious materials. *Magazine of Concrete Research*, **62**(11): 831–843, 2010.

[31] K. Van Tittelboom and N. De Belie. Self-healing concrete: suitability of different healing agents. *Internat J of 3R's*, pages 12–21, 2010.

[32] S.C. Olugebefola, A.M. Aragón, C.J. Hansen, A.R. Hamilton, B.D. Kozola, W. Wu, P.H. Geubelle, J.A. Lewis, N.R. Sottos, and S.R. White. Polymer microvascular network composites. *J. Compos Mater*, **44**(22): 2587–2603, 2010.

[33] J.W.C. Pang and I.P. Bond. A hollow fibre reinforced polymer composite encompassing self-healing and enhanced damage visibility. *Compos Sci Technol*, **65**(11): 1791–1799, 2010.

[34] R.S. Trask and I.P. Bond. Biomimetic self-healing of advanced composite structures using hollow glass fibres. *Smart Mater Struct*, **15**(3): 704–710, 2006.

[35] K.S. Toohey, N.R. Sottos, J.A. Lewis, J.S. Moore, and S.R. White. Self-healing materials with microvascular networks. *Nat Mater*, **19**(9): 1399–1405, 2007.

[36] K.S. Toohey, C.J. Hansen, J.A. Lewis, S.R. White, and N.R. Sottos. Delivery of two-part self-healing chemistry via microvascular networks. *Adv Funct Mater*, **19**(9): 1399–1405, 2009.

[37] D. Therriault. *Directed assembly of three-dimensional microvascular networks*. Univeristy of Illinois at Urbana-Champaign, 2003.

[38] D. Therriault, R.F. Shepherd, S.R. White, and J.A. Lewis. Fugitive inks for direct-write assembly of three-dimensional microvascular networks. *Advanced Materials*, **17**(4): 395–399, 2005.

[39] J.A. Lewis. Direct ink writing of 3D functional materials. *Adv Funct Mater*, **16**(17): 2193–2204, 2006.

[40] CubeX® Technical Specifications. `cubify.com/en/Products/CubeXTechSpecs`. Accessed: 21/05/2014.

[41] C.A. Harper and A. Baker. *Modern plastics handbook*. McGraw-Hill, New York, 2000.

[42] Permabond 101 Technical Data Sheet. `ellsworth.com/Resources/Technical-Data-Sheets/Permabond/Permabond-101-Technical-Data-Sheet/`. Accessed: 21/05/2014.

[43] Everbuild industrial superglue GP Technical Data Sheet. `everbuild.co.uk/image/data/Tech%20Adhesives/Industrial%20Superglue%20GP.doc`. Accessed: 21/05/2014.

[44] M.D. Abramoff, P.J. Magalhaes, and S.J. Ram. Image processing with ImageJ. *J. Biophotonics*, **11**(7): 36–42.

[45] Structures Data Book, *Cambridge Univesity Engineering Department*, 2008.

[46] Materials Data Book, *Cambridge Univesity Engineering Department*, 2008.

[47] A.T.T. Nguyen and A.C. Orifici. Structural assessment of microvascular self-healing laminates using progressive damage finite element analysis. *Composites Part A*, **43**(11): 1886–1894, 2012.

[48] K. Van Tittelboom, D. Van Loo, and N. De Belie. Evaluation of the efficiency of self-healing in concrete by means of u-ct. *Advances in Computed Tomography for Geomaterials: GeoX 2010*, page 132, 2013.

Appendix

Appendix A: *Risk Assessment Retrospective*

A risk assessment was submitted to the Health & Safety Office at the start of the project, identifying chemical, mechanical and office based hazards as issues to consider when formulating a safe system of work.

A dust mask was worn when working with cement powder; gloves, a lab coat and goggles were worn when handling cyanoacrylates and steel-cap boots were worn when tooling in the workshop and handling heavy concrete moulds. Due care was taken when using the 3D printer and universal testing machine.

The risk assessment adequately reflected the hazards present when undertaking a long term project involving these materials. No issues were reported.

	z-thickness = 100 µm		**z-thickness** = 250 µm		**z-thickness** = 500 µm	
ND (mm)	**OD** (mm)	**ID** (mm)	**OD** (mm)	**ID** (mm)	**OD** (mm)	**ID** (mm)
10.0	10.6	8.6	10.9	8.1	10.4	8.0
8.0	8.7	6.7	8.9	6.7	8.5	6.1
6.0	6.7	4.7	6.9	4.3	6.5	4.1
5.0	5.8	3.8	6.0	3.2	5.5	3.3
4.0	4.7	2.7	4.8	2.2	4.5	2.1
3.5	4.1	2.1	4.3	1.7	4.0	1.8

Appendix B: *Nominal (ND), Outer (OD) and Internal (ID) Diameters of printed tubes with varying layer thicknesses in the z-direction, measured before three-point bend testing.*

Tube Dimensions (mm) Nominal Diameter	Layer Thickness	**Failure Load (N)**	**Failure Displacement (mm)**	**Distance between crack and loading point (mm)**
10	0.1*	139.7	2.55	8.5
8	0.1*	99.3	3.28	10.5
6	0.1*	55.2	3.36	9.5
5	0.1*	—	—	—
4	0.1*	—	—	—
3.5	0.1*	17.3	5.57	8.0
10	0.25	181.5	3.23	10.5
8	0.25	110.5	3.83	15.0
6	0.25	67.5	5.6	9.0
5	0.25	38.9	4.89	9.0
4	0.25	30.2	11.34†	0.5
3.5	0.25	19.9	7.47	9.0
10	0.5	127.2	3.20	8.0
8	0.5	LOST	LOST	9.5
6	0.5	43.8	4.82	9.5
5	0.5	28.4	5.44†	0.0
4	0.5	21.8	9.02†	0.0
3.5	0.5	17.6	11.17†	1.0

Appendix C: *Load and central displacement at failure for tubes loaded in three-point bending. * Large structural "blobs" increase the thickness up to around 2.3 mm on the tensile side. † Tubes broke along the loading plane, not at the nearest support. The 0.1 mm layer thickness tubes were particularly fragile, and the ND5 and ND4 tubes broke when the print supports were removed, whilst the data file for the 0.5 layer thickness tube of ND8 was corrupted so failure load and displacement measurements were lost.*

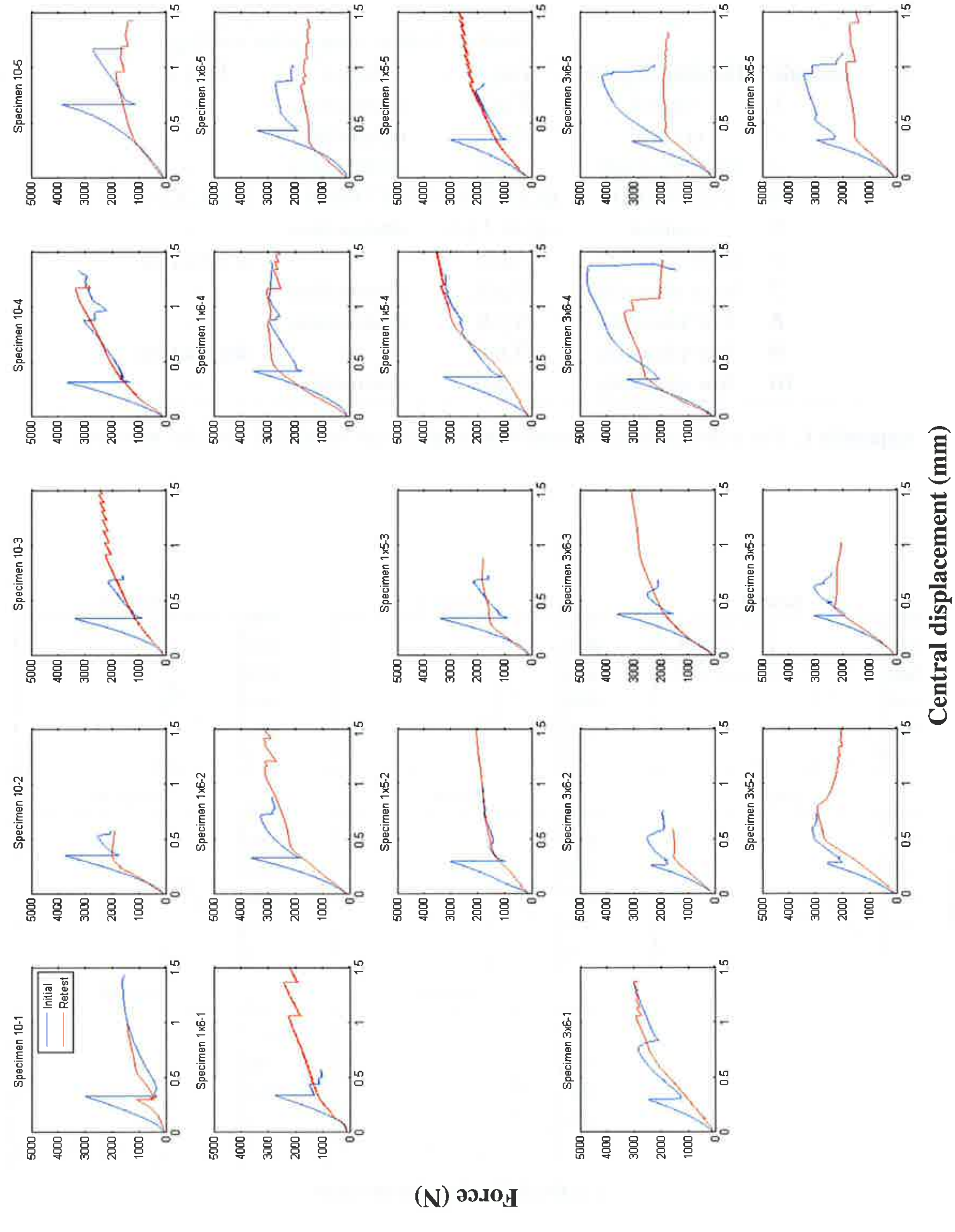

Appendix D: *Results of the tests on specimens with embedded tubes. The title prefix denotes the nominal diameter of the embedded tube(s), and the suffix describes the healing agent the tube(s) contained: (1) 1:1 cement paste, (2) 2:1 cement paste, (3) 3:1 cement paste, (4) high viscosity cyanoacrylate and (5) tracer dye used as a control. The chart with title "Specimen 1x6-2" therefore shows results from the specimen with a single 6 mm embedded tube filled with 2:1 cement paste. Samples which were blocked or did not leak are excluded.*

		Testing Action (days after curing)		
Sample	**Healing Agent**	Day 0	Day 1	Day 2
1	control	3 p.b.	destruction	—
2	control	3 p.b.	destruction	—
3	high viscosity	3 p.b.	destruction	—
4	NETWORK	BLOCKED	NETWORK	BLOCKED
5	control	offset 3 p.b.	destruction	—
6	high viscosity	3 p.b.	—	destruction
7	high viscosity	3 p.b.	destruction	—
8	low viscosity	3 p.b.	destruction	—
9	low viscosity	3 p.b.	—	destruction
10	low viscosity	3 p.b.	destruction	—

Appendix E: *The testing action performed on samples with embedded vascular networks.*

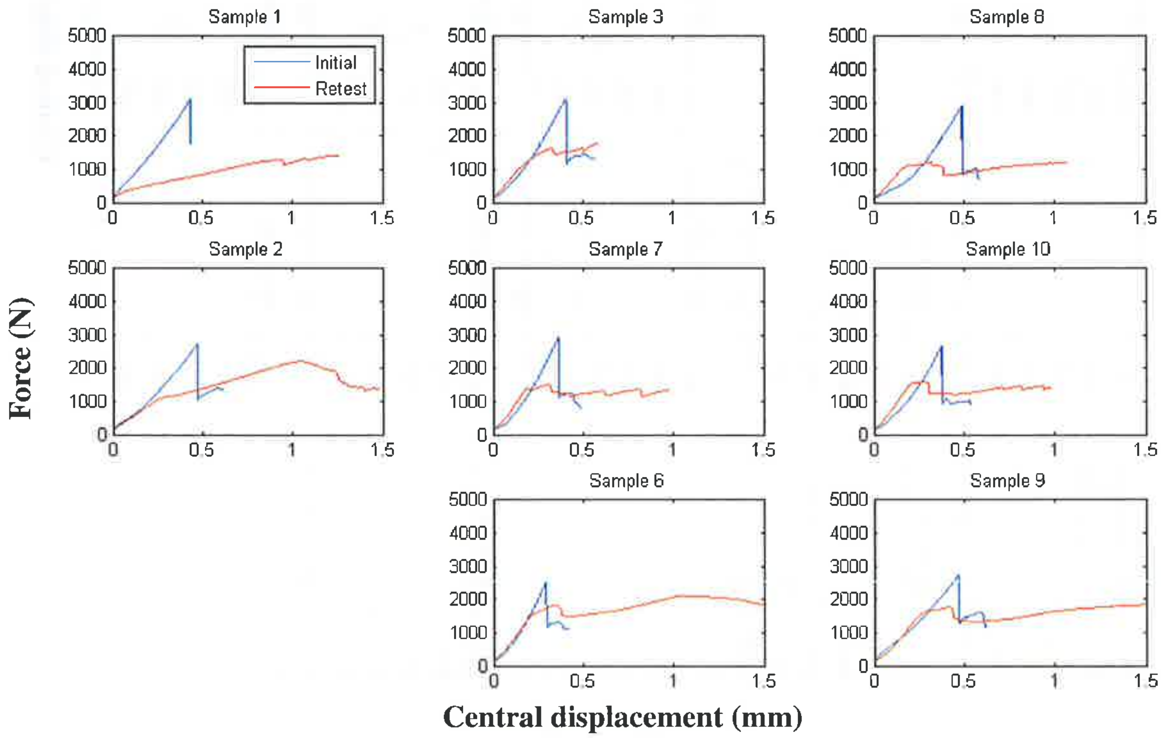

Appendix F: *Results of the tests on specimens with embedded vascular networks. Results along rows were left to heal for the same amount of time: (1) & (2) for one day, (3) for two days. Results along columns contained the same healing agent: (1) Tracer dye used as a control, (2) high viscosity cyanoacrylate and (3) low viscosity cyanoacrylate. The off-centre three-point bend control beam is excluded for the purposes of fair comparison.*